FINAL PROJECT REPORT

Impact of Climate Change in the Indus River Delta and Coastal Region of Pakistan

Dr. Altaf Ali Siyal

Dr. Zia ur Rehman Hashmi

CONTENTS

ACKNOWLEDGMENT

EXECUTIVE SUMMARY

Indus Delta, the 5th largest delta in the world, stretches from Sir Creek in the east to Phitti Creek in the west with the top at Banoo town district Sujawal, Sindh, Pakistan. This fan-shaped delta is one of the designated Ramsar wetland sites of Pakistan which supports the seven[th] largest mangrove ecosystem in the world in vast tidal mud floodplains. About 97% of the total mangrove forests of Pakistan are concentrated in the delta. Indus Delta, being near to the Arabian Sea, is threatened by increased seawater intrusion. Hence, huge agricultural lands have either simply become part of the sea or changed into salt affected with salt visible on the surface of the soils; hence are not suitable for agricultural practices. Most of the reports about the gravity of the problem are based on sampling surveys conducted from time to time without any scientific evidence and application of the latest scientific tools and techniques. Hence, significant variability in the data is observed about salt-affected soils and soil salinity conditions in the delta. Thus, data are usually not considered worth and hence do not get due considerations from the policymakers. Hence, keeping in view the above facts, the present study was planned to assess the status of soil salinity in the Indus delta using Remote sensing and geospatial tools. Also, develop a link between the availability of fresh water in the delta with changes in soil salinity so that to develop a strategic action plan for mitigation and adaptation measures to save the biodiversity of the delta, mitigate the adverse impact on the environment and other socio-economic conditions of people under current and future climate change scenarios.

The georeferenced soil samples from different soil depths were randomly collected from different locations of the delta. The soil samples were analyzed for different soil physicochemical properties. Also, EMI survey with EM38-MK2 was conducted of all sampled locations to validate with the laboratory results. The downstream Kotri barrage water flow data from 1937-38 to 2018 was collected from Sindh Irrigation Department. For spatial and temporal variation in the soil salinity of Indus delta, Landsat satellite imagery of last 29 years (from 1990 to 2018) were downloaded from the USGS Global Visualization Viewer (GloVis) and classified for the soil salinity in delta using soil salinity indices. SRTM Digital Elevation Model (DEM) of 30 m resolution of the Indus delta was acquired from the USGS EarthExplorer website for coastal flooding risk mapping.

The analysis of soil samples revealed that Indus delta is dominated with fine textured soils. It reflects that for all depths, the majority of soil textures had silty clay, clay loam, and loam textural classes. Thus, the soils of the delta are dominated with heavy fine-textured soils. The vast areas along the coastal belt had electrical conductivity of soil saturation extract (EC) greater than 15 dS/m, may be due to the impact of subsurface seawater intrusion. EC decreased significantly in areas located away from the sea. Most of the sampled soil had pH values within 8.5. However, the pH values of soil samples collected from and nearby tidal floodplains had higher values of pH. The interpolated soil salinity maps showed that more than 80% of the land in Indus delta was salt-affected. While the irrigated salt affected land has increased from 57.4% to 57.7% of the delta during the last three decades. Whereas, the area under normal soil decreased from 29.3% of the delta to 26.7% during the same period. After construction of dams and barrages over the Indus River system, the average annual discharge of water and sediment below Kotri Barrage has decreased significantly especially after the year 2000. Zero-flow days started after commissioning of Kotri and Guddu Barrages during 1962-1967. Currently, downstream Kotri Barrage flow is constrained mainly within only two months of monsoon, i.e., August-September.

There was a negative and weak relation between the volume of water released below Kotri barrage and the area under salt affected soils with a coefficient of determination of $R^2 = 0.483$. However, the relation was positive with a coefficient of determination of $R^2 = 0.370$ between the Kotri downstream flow and the normal soil area. It reflects that with an increase in flow below Kotri downstream, there is a slight increase in the normal soil and thus decrease in soil salinity.

A low-elevation coastal zone (LECZ) having an elevation below 10 m spreads over vast areas of the delta. Analysis of DEM portrays that about 94% of the delta or 12250 sq. km of delta fall within the LECZ; thus, highly vulnerable to coastal inundation. Almost, all major cities of the delta are located in LECZ, hence are under high risk of coastal flood inundation. The degradation, shrinking, and coastal flooding of Indus delta has a significant impact on the environment and the economic conditions of the delta. It is estimated the economic cost of degradation of the Indus Delta around US\$2 billion annually. If average rice crop yield is 60 Maunds per acre and price per maund is Rs. 1000, then the agricultural economic loss of delta due to coastal flooding in Kharif season could be estimated as much as Rs. 30 billion. Similarly, If the coastal flooding occurs during Rabi season, the agricultural loss could be estimated as Rs. 27 billion. Except for agricultural loss, environmental, ecological and infrastructure losses would also be severe.

Based on present study it is recommended that:

- Biosaline agriculture should be introduced and encouraged by the government in tidal floodplains and over the vast barren salt-affected soils lying between tidal floodplains and the canal irrigated areas of the delta especially on the left bank of river Indus. Pal grass, Quinoa, Salicornia, Sea Aster, Spartina alterniflora, etc. have a bright scope of cultivation and high yield in these areas. Biosaline agriculture will certainly be a source of food and fodder for the coastal communities and livestock. Thus, it will help in the mitigation of poverty and in improving the coastal environment under changing climate scenario.
- A 38 km long coastal highway constructed at the periphery of the tidal floodplain on the right bank of Indus should be extended 180 km further on the left bank of Indus by putting a bridge over the river Indus at Kharo Chhan. The proposed highway will not only provide coastal communities with quick and easy access to the markets of Karachi but will also attract the tourists and flourish tourism in the delta. Hence, socio-economic conditions of poor communities of the delta will be improved. Also, it will act as a defense-line against the surface seawater intrusion, thus will impede further swallowing of the delta by sea. It will also act as barrier against coastal flooding due to tsunami, cyclone or any other natural disaster.
- As per recommendations of International Experts (IPOE) in 2004; water flow of 5000 cusecs throughout the year should be ensured below Kotri Barrage to minimize the impact of seawater intrusion and meet the environmental flow needs flora and fauna. Also, a total volume of 25 MAF in five years (equivalent to 5 MAF annually) be released below Kotri barrage as flood flows (Kharif period).
- For minimizing surface and subsurface seawater intrusion in the entire delta, sufficient water in canals originating from Kotri Barrage should be ensured along with the environmental flow in the river. It will not only minimize seawater intrusion but also provide drinking water to coastal communities and mitigate adverse impacts on the ecosystem of the delta. Satellite images provide evidence that irrigation channels of the delta have a significant impact on the seawater intrusion in areas far from the river Indus.
- If possible, old relic river channels, such as Ochito and Old Pinyari, should be restored. These channels, if restored, will carry extra flood water to the sea during a high flood and thus shun the pressure on the levees of the main river and thus minimize the possibility of the levee

breach. It will also supply fresh water to the coastal communities living far away from the main river course.

- Most of the natural lakes in the delta are saline, which should be revitalized by adding freshwater during the monsoon period. Freshwater lakes can play a vital role in providing drinking water to the communities and also work as groundwater recharge hotspots.
- Tourism Industry should be encouraged in the delta, especially boat cruising in the mangrove laden creeks in the Delta to improve socioeconomic conditions of poor local communities

ACRONYMS

AOI	Area of Interest
BCM	Billion Cubic Meters
DEM	Digital Elevation Model
DN	Digital Numbers
dS/m	Deci Siemens per meter
EC	Electrical Conductivity
EMI	Electromagnetic Induction
ESP	Exchangeable Sodium Percentage
ETM	Enhanced Thematic Mapper
GIS	Geographical Information System
GLoVIS	Global Visualization Viewer
GPS	Global Positioning System
ha	Hectare
IPCC	Intergovernmental Panel on Climate Change
IDW	Inverse Distance Weighted
MAF	Million Acre Feet
mg	Milligrams
mg/L	Milligram/Liter
MSS	Multispectral Scanner System
NDSI	Normalized Difference Salinity Index
OLI	Operational Land Imager
PMD	Pakistan Meteorological Department
ppm	Parts per million
R^2	Coefficient of determination
SAR	Sodium Adsorption Ration
SI	Salinity Index
TDS	Total Dissolved Solids
TM	Thematic Mapper
TOA	Top of atmospheric
USGS	United States Geological Survey

WHO	World Health Organization
WRS	World Reference System
WWF	World Wide Forum for Nature
A_L	Band-specific additive rescaling factor
$\rho\lambda'$	Top of atmospheric (TOA) planetary reflectance, without correction for the solar angle.
$M\rho$	Band-specific multiplicative rescaling factor
$A\rho$	Band-specific additive rescaling factor
$Qcal$	Quantized and calibrated standard product pixel values (DN)
ρ_λ	TOA planetary reflectance
θ_{SE}	Local sun elevation angle
θ_{SZ}	Local solar zenith angle
L_λ	Top of Atmosphere spectral radiance
M_L	Band-specific multiplicative rescaling factor
Q_{cal}	Quantized and calibrated standard product pixel values
K_1	Band-specific thermal conversion constant
K_2	Band-specific thermal conversion constant
T	At-satellite brightness temperature (K)

LIST OF TABLES

LIST OF FIGURES

1. INTRODUCTION

Indus Delta, is the 5th largest delta (IUCN, 2003; Sohl, et al. 2006; WWF, 2010; Khan and Akbar, 2012; Baig et al., 2017) in the world which stretches from Sir Creek in the east to Phitti Creek in the west with the top at Banoo town district Sujawal, Sindh, Pakistan. This fan-shaped delta is a designated Ramsar wetland site of Pakistan which supports seven[th] largest mangrove system in the world in vast tidal mud floodplains (Amanullah et al., 2014; WWF, 2010; Sultana et al., 2014; Baig et al., 2017). Mangrove forest system of the Indus delta is no doubt largest mangrove system in the arid regions of the world (Hecht, 1999; Hamid et al., 2000; Mimura, 2008; Ismail et al., 2014). About 97% of the total mangrove forests of Pakistan are concentrated in the delta. Nearly 95% of the total mangrove forests contain *Avicennia marina* species (WWF, 2007). It provides a livelihood to nearly 0.9 million coastal population (Wood et al., 2013). It is reported that Indus delta is one of the world's most vulnerable large deltas (Spalding et al., 2010). Due to decrease in the river flows to the delta, subsurface seawater intrusion, sea level rise, low rainfall due to climate change and anthropogenic activities, one of the largest ecosystems of the world is shrinking and degrading at an alarming rate (Majeed et al., 2010; Rasul et al., 2012). The strong monsoonal winds create high wave energy levels. The river Indus ranks 4th position in a wave power at the deltaic shoreline among all the rivers of the world of about 13 joules/sec/unit crest width. While at a distance from the shoreline where the water depth is 10 m, the wave power generated is about 950 joules/sec/unit crest width (Mimura, 2008). Thus, the delta is exposed to the strongest wave action of any river delta in the world (Mimura, 2008). It is reported that the Indus delta receives more amount of wave energy per day compared to that received annually by the Mississippi River Delta (Giosan et al., 2006; Mimura, 2008). Until the construction of hydraulic structures on the Indus river system, the delta sustained this wave action due to freshwater flow below Kotri barrage to mitigate the erosional impact of waves.

In coastal areas, soil salinization is a common and serious problem affecting crop cultivation and ecology of the delta (Yu et al., 2014). Indus Delta, being near to the Arabian Sea, is threatened with increased seawater intrusion. Hence, massive agricultural lands have either become part of the sea or changed into salt affected with salt visible on the surface of the agricultural lands and hence are not suitable for agricultural practices. The mapping of soil salinity using GIS and Remote sensing with different vegetation and salinity indices provide a simple and easy way of knowing how much

of damage has been occurred to the delta due to soil salinity and what could be done for the prevention of ecological degradation (Asfaw et al., 2018)

Since the last few decades, deltas of the world are under threat of sea-level rise (SLR), resulting from subsidence, glacier melt, and other extreme meteorological events. It places the ecosystems and human populations living in deltas at risk (Schneider et al., 2007) and will destroy most of the deltas of the world in the next century (Giosan et al., 2014). IPCC (2007) reported that the sea level rose about 15-20 centimeters or roughly 1.5 to 2.0 mm/year during the last century. The IPCC has also projected that sea level will likely rise by 21 to 71 cm by the year 2070 with the best estimate of 44 cm. This will certainly inundate the coastal areas of the delta. Moreover, due to the flat topography of delta, future tsunamis and cyclones will have a larger impact on Delta, which might cause irreparable loss to Pakistan. Thus, coastal flood mapping is vital for hazard planning and management and mitigation of impacts of sea level rise due to climate change or other natural hazards such as tsunamis, cyclones, etc.

So far reports available on the gravity of soil salinity and natural hazard problems are based on soil sampling surveys conducted time to time without any scientific evidence and application of latest scientific and geospatial tools and techniques. Hence, significant variability in the data is observed about salt-affected soils and soil salinity conditions in the delta. Without any scientific approach/evidence, these reports are usually not considered worth and hence do not get due considerations from the policymakers. Hence, keeping in view above facts the present study was planned to assess the status of soil salinity in the Indus delta using Remote sensing and geospatial tools and develop a link between availability of fresh water in the delta with changes in soil salinity so that to develop a strategic action plan for mitigation and adaptation measures to save the biodiversity of delta, mitigate adverse impact on environment and other socio-economic conditions of people under current and future climate change scenarios.

The outcome of the present study certainly provide a constructive foundation for policymakers, analysts, and researchers to devise a strategic action plan for mitigation of salinity hazard in the Delta. The articulation of land reclamation measures will not only be constructive and favorable for the ecosystem but also will revamp the socio-economic conditions of the local communities.

1.1   Location

The Indus delta is located the tail end of river Indus in the southern province of Pakistan. It stretches from Longitude 67°11'9.76" E to 68°44'46.23" E and latitude from 23°47'25.20" N to 24°57'30.90" N (Fig. 1.1). The Indus delta mangrove ecosystem is unique, and the only arid mangrove system of Asia, which is highly resistant to extreme temperatures, seawater salinity, and low precipitation (DasGupta and Shaw, 2013). Mangroves play a vibrant role in the protection of coastline against erosion by acting as a natural barrier during storm surges. The natural vegetation in the tidal floodplains of the delta contains varying degrees of mangrove forests (Leichenko and Wescoat, 1993).
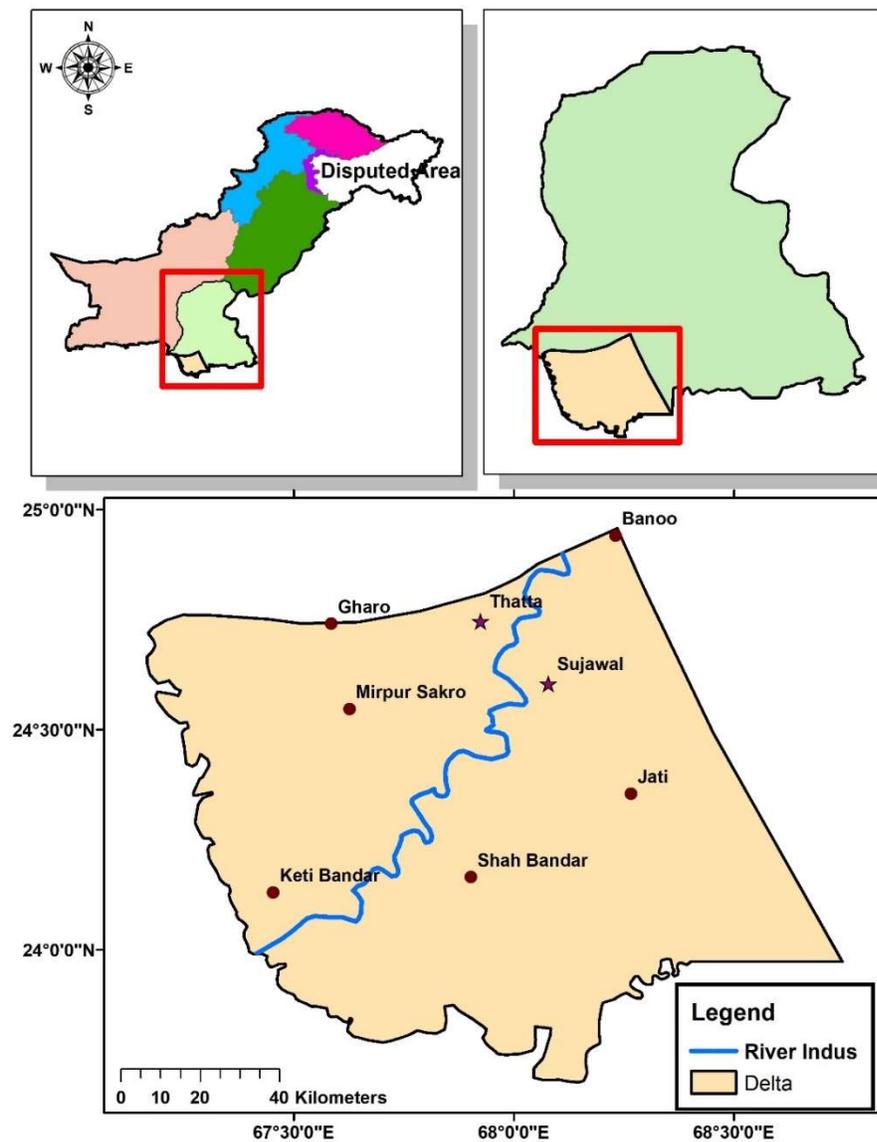
Fig. 1.1: Location map of Indus Delta

1.2 Climate of delta

The delta is an arid region with a mean annual rainfall of less than 200 mm (Mimura, 2008; Giri et al., 2015); whereas average temperatures in the delta range from 23.8 to 28.7 °C (IUCN, 2002; Majeed et al., 2010; Kalhoro et al. 2016). About 80% of the rain in the delta falls during the monsoon period (June-September). During the summer, the delta receives intense southwest monsoonal winds. While in the winter the delta gets colder northeasterly winds.

1.3 Coastal Flooding

The rise in sea level rise affects the coastline in two different ways, i.e. by inundation, and by coastal erosion (Steffen et al., 2014). The coastal inundation or flooding is the process by which the rise in sea level inundates the coastal land, without any change of the actual land surface. While the coastal recession is the process in which sandy or muddy shoreline is eroded landwards under a rising sea level. The inundation of coastal areas is due to seawater above normal tidal actions. It is often caused by strong winds, tsunamis, and high lunar tides. Climate change poses many hazards to coastal ecology, morphology, and the environment. Main of among these risks is sea level rise. It threatens the human population, ecosystems, and the coastal infrastructure directly and also amplifies the impacts of coastal cyclones. During the late 19th century, the rate of sea level rise was about 0.6 mm per year (Church and White, 20011) which increased to approximately 1.8 mm per year (Miller and Douglas, 2004) in the second half of the 20th century. It is estimated that during the 20th century, the global average sea level has risen by 17 cm (Steffen et al., 2014). The rate of sea level rise increased further to 3 mm per year during the 1st decade of the 21st century (Vermeer and Rahmstorf, 2009) as shown in Fig. 1.2. The Intergovernmental Panel on Climate Change (IPCC) has projected that the sea level would further rise 0.18 to 0.59 m by the end of the 21st century (Meehl et al., 2007). Horton et al. (2008) projected a sea level rise of 0.62 to 0.88 m by 2100. Rohling et al. (2008), based on paleoclimatic evidence, investigated that a sea level rise rate of 1.6 m per century is possible. Coastal flooding is called a sleeping giant (Steffen et al., 2014). If the risk of sea level rise is ignored, then the projected economic damages resulting from coastal flooding are enormous. Thus, policymakers, coastal managers, environmentalists, governments, and local population are all concerned about current and future menaces to coastal areas due to climate change and anthropogenic activities.

The topography of Indus delta is flat; the elevation of most of the delta ranges between 0 to 20 m. Thus, it is most vulnerable to impacts of sea level rise, *viz.* costal erosion and flooding, under changing climate change scenario. Hence, mitigation measures for the risks posed by climate change and sea level rise should be initiated before the collapse of ecology, morphology, and the environment of coastal areas.
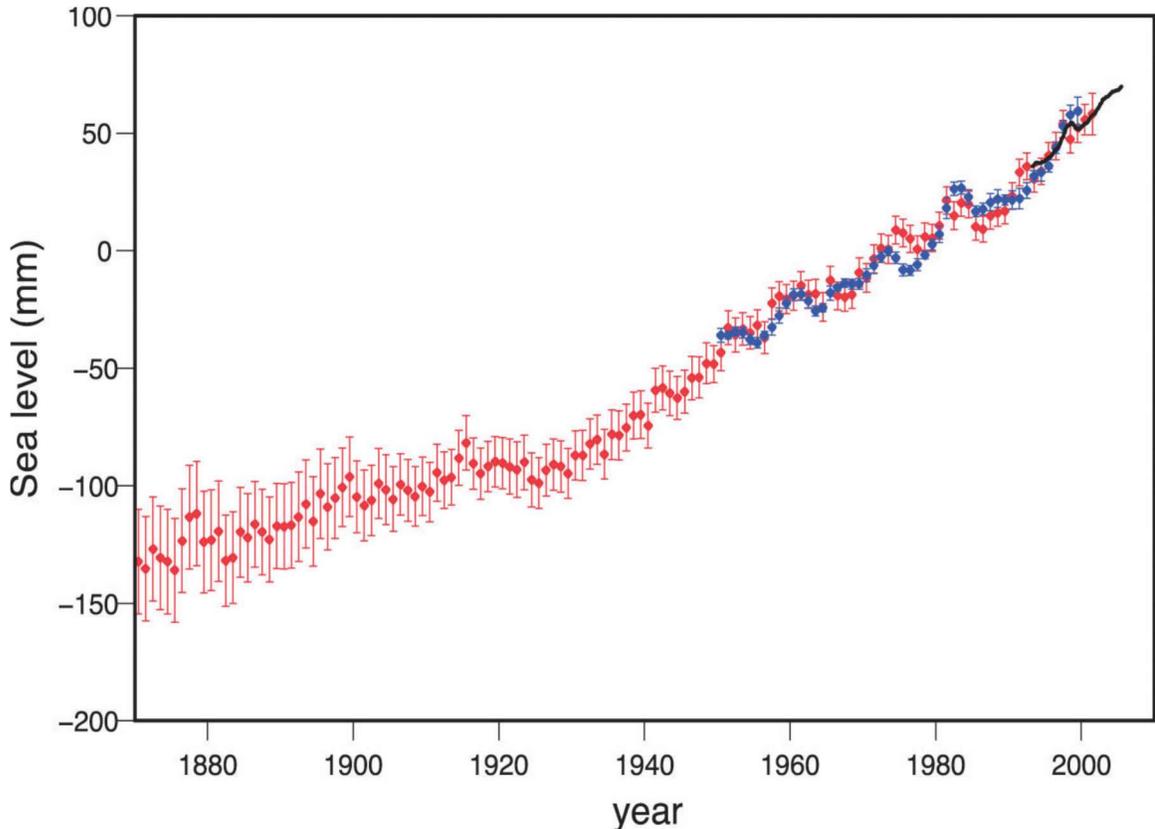
Fig. 1.2: Temporal variation in annual, global mean sea level rise (source: Steffen et al., 2014)

About 2% of the land surface are coastal areas having elevation less than 10 m above mean sea level (MSL). While about approximately 10% of the population of the earth lives in the 10 m elevation coastal zone (Nicholls, 2004; Van et al., 2012; Neumann et al., 2015). Population concentrations in low-elevation areas are even greater in developing countries. It has been estimated that 93 to 310 million inhabitants are settled at elevations having less than 100-year flooding event (Hinkel, 2013).

1.4   Delineation of Indus Delta

Different figures about the area of Delta are cited in the literature by different researchers (Table 1.1). Hence, it was difficult to decide which area to consider for the present study. Thus, for the present technical study, the first and the most difficult task was a delineation of the boundaries of Indus delta for the collection of the required data.

Table 1.1: Area of the Indus Delta (Review of Literature)

S. No.	Area		Reference
	sq. km	Hectares	
1	6,000	6,00,000	Meynell and Qureshi (1993); Khan and Akbar (2012); Giri et al. (2015); Memon (2005);
2	8,500	8,50,000	Ahmed and Shaukat (2015)
3	30,000	30,00,000	Leichenko et al. (1993); Renuad et al. (2013)
4	17,000	17,00,000	Syvitski et al. (2013)
5	16,000	16,00,000	Callaghan (2014)
6	41,440	41,44,000	Peracha et al. (2015)
5	5,000	5,00,000	Laghari et al. (2015)

To delineate the delta based on some historical evidence, old maps of Talpur (1833) and British era (1893) were collected (Fig. 1.3). During those days, on the left bank of the river Indus, the Pinyari river/estuary originated from river Indus near Banoo town (District Sujawal) and discharged into the Arabian sea via Sir Creek in the east. Considering the Banoo town as an apex of the delta while Sir Creek and Phitti Creeks as two base points of the delta in the east and west respectively, the Indus delta was delineated as shown in Fig. 1.4.
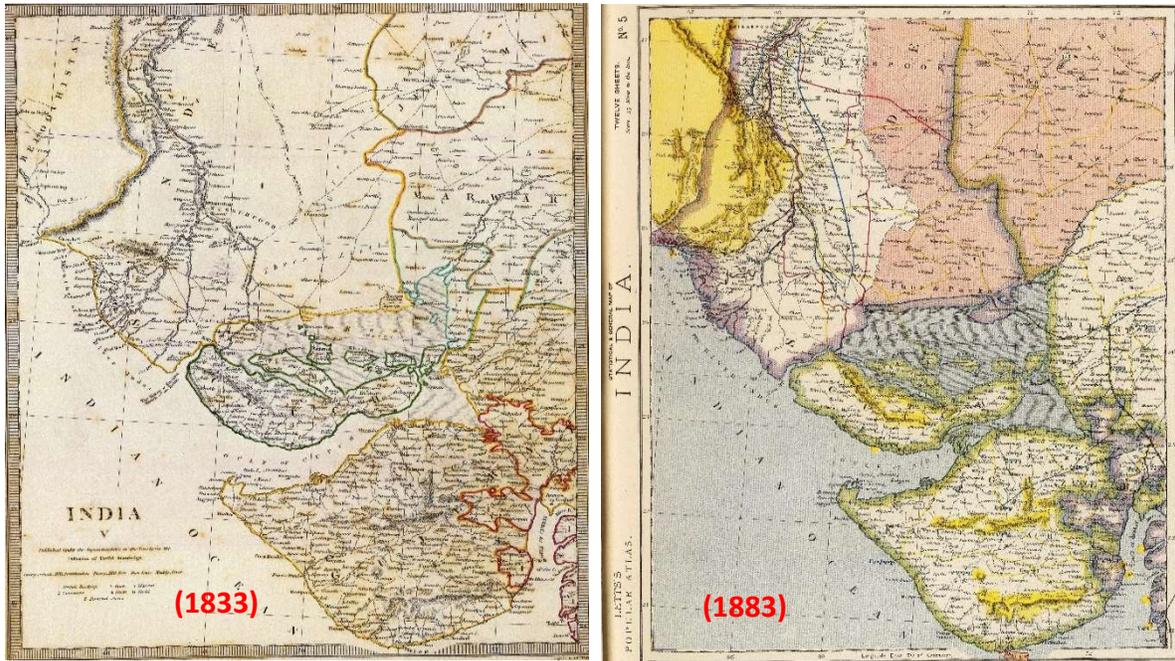
Fig. 1.3: Maps of Sindh during the Talpur era (1833 AD) and British era (1883 AD) showing Pinyari river off taking from river Indus at Banoo Town

The Indus delta delineated for the present study stretches over an area of about 13067 sq.km (1.3 Mha). It covers almost the entire geographical boundaries of the Sujawal and Thatta districts except for the mountainous part of the Thatta district.
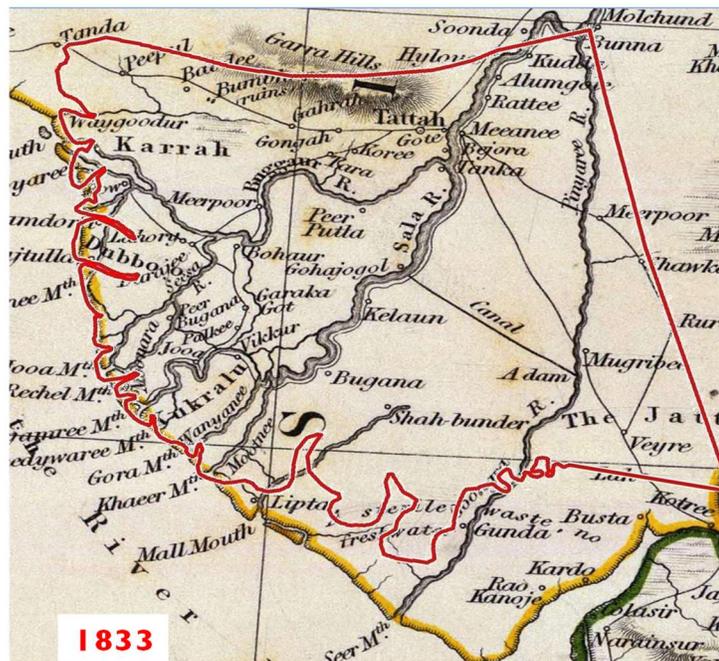
Fig. 1.4: Delineation of the Indus Delta (based on a map of Sindh 1833 AD)

2. MATERIALS AND METHODS

2.1 Spatio-temporal analysis of variation in soil salinity levels in the Indus delta using the field and remote sensing data

2.1.1 Soil Sampling

The georeferenced soil samples from 0-20, 20-40, and 40-60 cm of soil depth were randomly collected from different locations of the all union councils within boundaries of the delta (Fig. 2.1 and Fig. 2.2). The soil samples were manually collected using soil auger. The location of the sampling points was recorded using the handheld Garmin GPS (GPSMAP 62S). Total 450 soil samples from 150 different locations of the study area were collected and analyzed for various physicochemical parameters *viz*. texture, electrical conductivity (EC), hydrogen ion concentration (pH) and exchangeable sodium percentage (ESP).
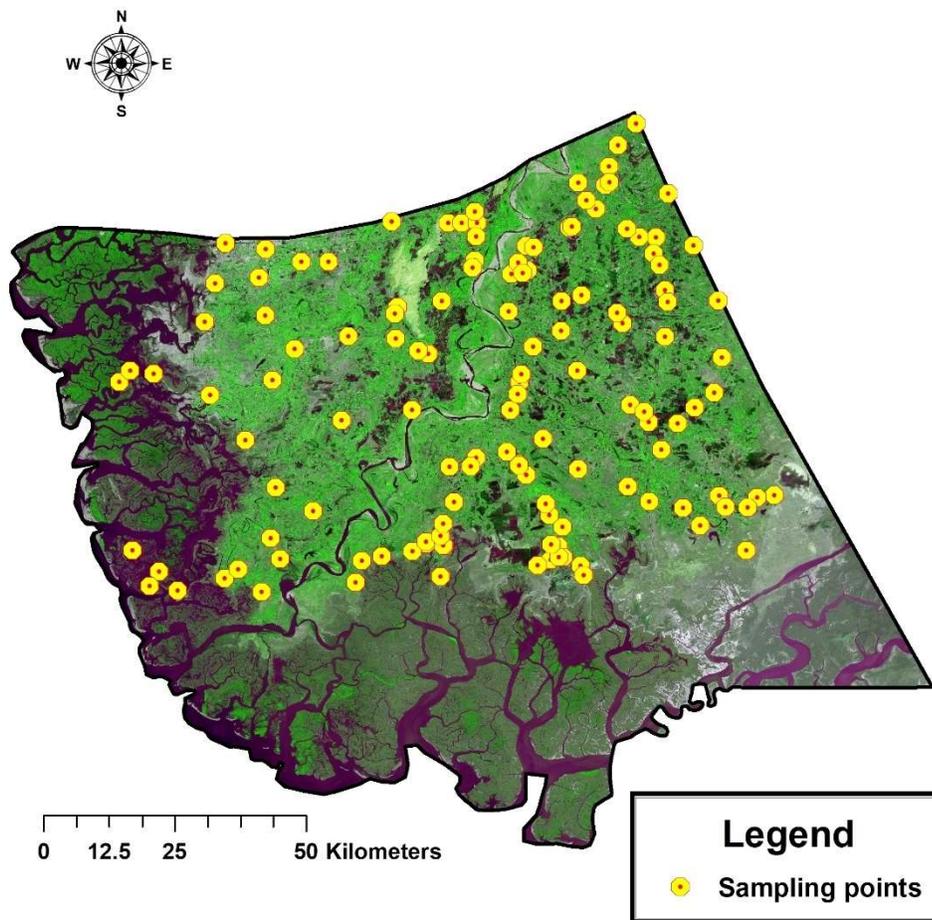
Fig. 2.1: Spatial distribution of soil sampling locations in the Delta

Fig. 2.2: Snapshots taken during soil sampling from Indus Delta

2.1.2 Physicochemical Analysis of Soil samples

Soil particle size distribution of all samples was determined by Bouyoucos method using a hydrometer (Bouyoucos, 1936). Soil textural class was determined using the soil textural triangle suggested by USDA (Gee and Or, 2002). Oven drying method was used for determination of the dry density of the soil samples. The electrical conductivity of soil saturation extract (EC) of the soil samples was determined at 25 ^{0}C using digital EC meter (Pessoa et al., 2016). The pH of soil saturation extracts was measured using pH meter. Sodium concentration in the soil was determined using flame photometer while the cations Ca^{+2} and Mg^{+2} were determined using titration method. Na^{+1}, $Ca^{+2,}$ and Mg^{+2} were used to calculate the sodium absorption ratio (SAR). From SAR, the exchangeable sodium percentage (ESP) was calculated.

2.1.3 EMI survey

A laboratory method for determining of the soil salinity includes soil sampling from the field, preparation of soil saturation paste and electrical conductivity of the soil saturated solution extract. The methods are time-consuming, laborious, and expensive, and provide only a limited number of point measurements that may not be representative of the entire field (Doolittle and Brevik, 2014). Due to the high spatial variability in soil salinity, the traditional method, though reasonably accurate, but have limited data points for the assessments of soil salinity at field and regional level (Corwin, 2008). While the Electromagnetic Induction (EMI) techniques produce many georeferenced, quantitative and in-situ measurements of the soil salinity, which could provide a better picture of the spatial variability of salinity at the field and larger scales. Thus, for rapid soil salinity survey and mapping, EMI survey has advantages over traditional methods (Doolittle and Brevik, 2014).

For the present study, Geonics EM38-MK2 was used in EMI survey of the Indus Delta. Soil salinity was also determined with EM38-MK2 at all those 150 places from where soil samples were collected to reconfirm and validate the EMI survey (Fig. 2.3).

Fig. 2.3: Snapshots of the EMI survey of Indus Delta

2.1.4 Mapping of Soil Salinity

Based on the EMI survey and analysis of the soil data, thematic maps for various physicochemical parameters *viz*., electrical conductivity (EC), soil pH, exchangeable sodium percentage (ESP), texture were prepared using ArcGIS 10.3 software. Spatial analysis 'Inverse Distance Weighted (IDW)' interpolation approach was used to develop the spatial distribution thematic maps. Based on physicochemical analysis of the soil samples, the delta was mapped with four soil salinity classes, i.e., as normal (non-saline), saline, sodic or alkali and saline-sodic soils.

2.1.5 Landsat imagery

For spatial and temporal variation in the soil salinity of Indus delta, Landsat satellite imagery of last 29 years (from 1990 to 2018) were downloaded from the USGS Global Visualization Viewer (GloVis) and classified for quantification of the soil salinity. The satellite imagery used for the analysis is summarized in Table 2.1. The area of interest (AOI), i.e., Indus Delta is covered in two tiles of the satellite image. Hence the two satellite images having WRS (World Reference System) paths 151 and 152 and row 43 were mosaicked first and then the AOI was extracted from the entire scene using shapefile of the delta as a mask in "extract my Mask" tool in spatial analyst toolbox of ArcGIS 10.5. The digital numbers (DN) of visible, near infrared of the AOI were first converted to radiance and then to Top of Atmospheric Reflectance (ToA$_r$) through the techniques described by Chander et al. (2009) and Siyal et al. (2015) using equations 1 and 2.

$$\rho\lambda' = M\rho Qcal + A\rho \qquad (2.1)$$

and

$$\rho\lambda = \frac{\rho\lambda'}{\cos(\theta_{SZ})} = \frac{\rho\lambda'}{\sin(\theta_{SE})} \qquad (2.2)$$

where:

$\rho\lambda'$ = Top of atmospheric (TOA) planetary reflectance, without correction for the solar angle.

$M\rho$ = Band-specific multiplicative rescaling factor from the metadata

$A\rho$ = Band-specific additive rescaling factor from the metadata

$Qcal$ = Quantized and calibrated standard product pixel values (DN)

ρ_λ = TOA planetary reflectance

θ_{SE} = Local sun elevation angle. The scene center sun elevation angle in degrees is provided in the metadata (SUN ELEVATION).

θ_{SZ} = Local solar zenith angle; θ_{SZ} = 90° - θ_{SE}

Table 2.1: Landsat satellite imagery (from 1990 to 2019) used for the vegetation analysis

S. No	Year	Acquisition date	Path	Row	DOY	d	θ$_s$
1	1990	Feb. 10	151[a]	43	41	0.98680	37.253531
2		Feb. 17	152[a]		48	0.98814	38.963608
3	2000	Feb. 14	151[b]	43	45	0.98755	43.035698
4		Feb. 05	152[b]		36	0.98596	40.742568
5	2010	Feb. 09	151[b]	43	40	0.98662	41.729947
6		Feb. 16	152[b]		47	0.98794	43.632710
7	2015	Feb. 15	151	43	46	0.98774	44.458135
8		Feb. 06	152		37	0.98612	42.059338
9	2019	Feb. 10	151[c]	43	42	0.98698	43.081681
10		Feb. 01	152[c]		31	0.98523	40.892219

[a] Landsat 5;   [b] Landsat 7;   [c] Landsat 8

2.1.6 Salinity Indices

Remote sensing and geospatial tools are widely used for the identification and delineation of salt-affected soils. Ghabour and Daels (1993) reported that detection of soil salinity through conventional methods of soil surveying requires time, labor and money but remote sensing data and techniques offer the possibility for mapping soil salinity efficiently and economically. The most commonly used technique for determining soil salinity is the calculation of different indices and ratio images using infrared and visible spectral bands of satellite data. Following salinity, indices were used in the present to delineate the salt-affected areas of the delta.

i.   Normalized Difference Salinity Index = $NDSI = \dfrac{red - nir}{red + nir}$ (Khan et al., 2005)

ii.   Salinity Index-1 = $SI = \sqrt{blue \text{ x } red}$ (Khan et al., 2001)

iii.   Brightness Index = $BI = \sqrt{(red)^2 \text{ x } (nir)^2}$ (Khan et al., 2005)

2.1.7 Tools used in the study

Following tools/software/data used to accomplish the objective 1 is given below:

1. Geonics EM38-MK2   2. Garmin GPSMAP 62S

3. Soil Augur   4. Core Samplers

5. Landsat Satellite Imagery (ETM, ETM+, OLI) 6. SRTM DEM (30 m)

7. ArcGIS 10.3

2.2 Developing a linkage/relation of the current soil salinity profiles (observed spatially and vertically using state of the art field equipment/instruments) with the changes in freshwater supplies downstream of Kotri

For the development of the link between the temporal and spatial variation in soil salinity and water flow downstream of Kotri barrage, the secondary data of annual inflow of the river to the delta from 1937-38 to 2018 was collected from Sindh Irrigation Department. Also, the data about the number of days per year with no or zero flow from 1956-57 to date below Kotri Barrage were collected and analyzed in Excel spreadsheets. A linkage/relation in terms of regression equation between the availability of river flow in delta with the temporal variation in soil salinity, determined through field and satellite data, was developed.

2.3 Coastal area inundation under different sea level rise scenarios and estimation of associated environmental/economic loss.

2.3.1 Digital Elevation Model (DEM)

The areas of delta vulnerable to coastal flooding were mapped using NASA's Shuttle Radar Topography Mission (SRTM) DEM (Digital Elevation Model) of 30 m resolution. For this, the DEM of the Indus delta was acquired from the USGS website https://earthexplorer.usgs.gov/. The study area is covered in four tiles DEMs. The metadata of the tiles is given in Table 2.2.

Table 2.2: Metadata of SRTM DEM used in the study

S. No	ID	EXTENT				Pixel Depth	Col.	Rows
		Top	Left	Right	Bottom			
1	n23_e067_1arc_v3	24.0001388889	66.9998611111	68.0001388889	22.9998611111	16 Bit	3601	3601
2	n23_e068_1arc_v3	25.0001388889	67.9998611111	69.0001388889	23.9998611111	16 Bit	3601	3601
3	n24_e067_1arc_v3	25.0001388889	66.9998611111	68.0001388889	23.9998611111	16 Bit	3601	3601
4	n24_e068_1arc_v3	25.0001388889	67.9998611111	69.0001388889	23.9998611111	16 Bit	3601	3601

2.3.2 DEM processing in ArcGIS

The DEM tiles were mosaicked to a single raster using "Mosaic to New Raster" in Toolbox of the ArcGIS 10.5 first, and then the area of interest (AOI), i.e., Indus delta was extracted using the shapefile of the delta as a mask in "Extract by Mask" tool as shown in Fig. 2.4.
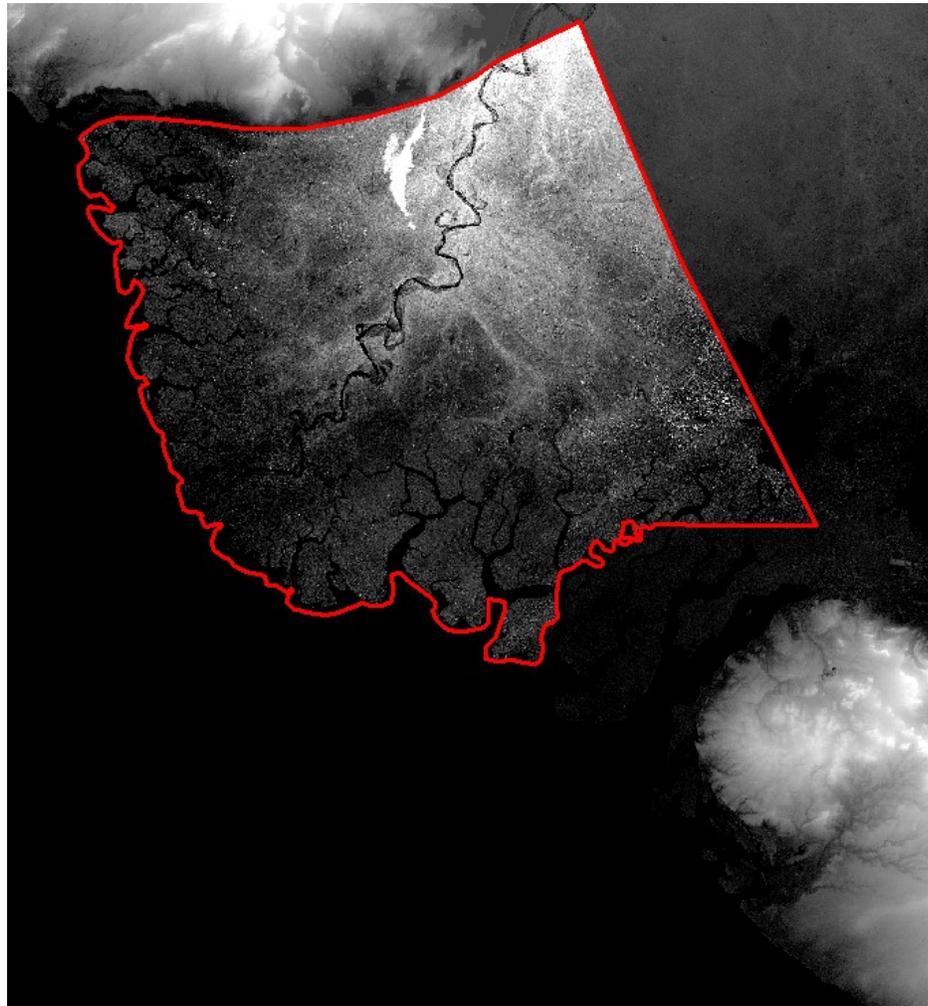
Fig. 2.4: Mosaicking of tiles and extraction of AOI (Indus Delta)

The extracted DEM of the AOI was analyzed in ArcMap and ArcScence and categorized into sea flood risk areas by classifying it into different classes based on the elevation of the area assuming different sea level rise scenarios, a tsunami wave or a cyclone capable of rising the sea level at different heights.

3. RESULTS AND DISCUSSIONS

3.1 Spatio-temporal analysis of variation in soil salinity levels in the Indus delta using the field and remote sensing data

3.1.1 Soil texture

The distribution of soil particles at 0-20, 20-40, and 40-60 are graphically presented in Fig. 3.1 (a, b and c), respectively. It reflects that for all depths, the majority of soil particles fall within silty clay, clay loam, and loam textural classes. It might be because of the location of the Indus delta at the tail end of the river Indus. As the coarse-textured sediment is deposited in upper regions while the river brings sediment dominated with fine particles at the tail end. Majeed et al. (2010) also reported that most of the soil in the Indus delta were heavy textured soils.
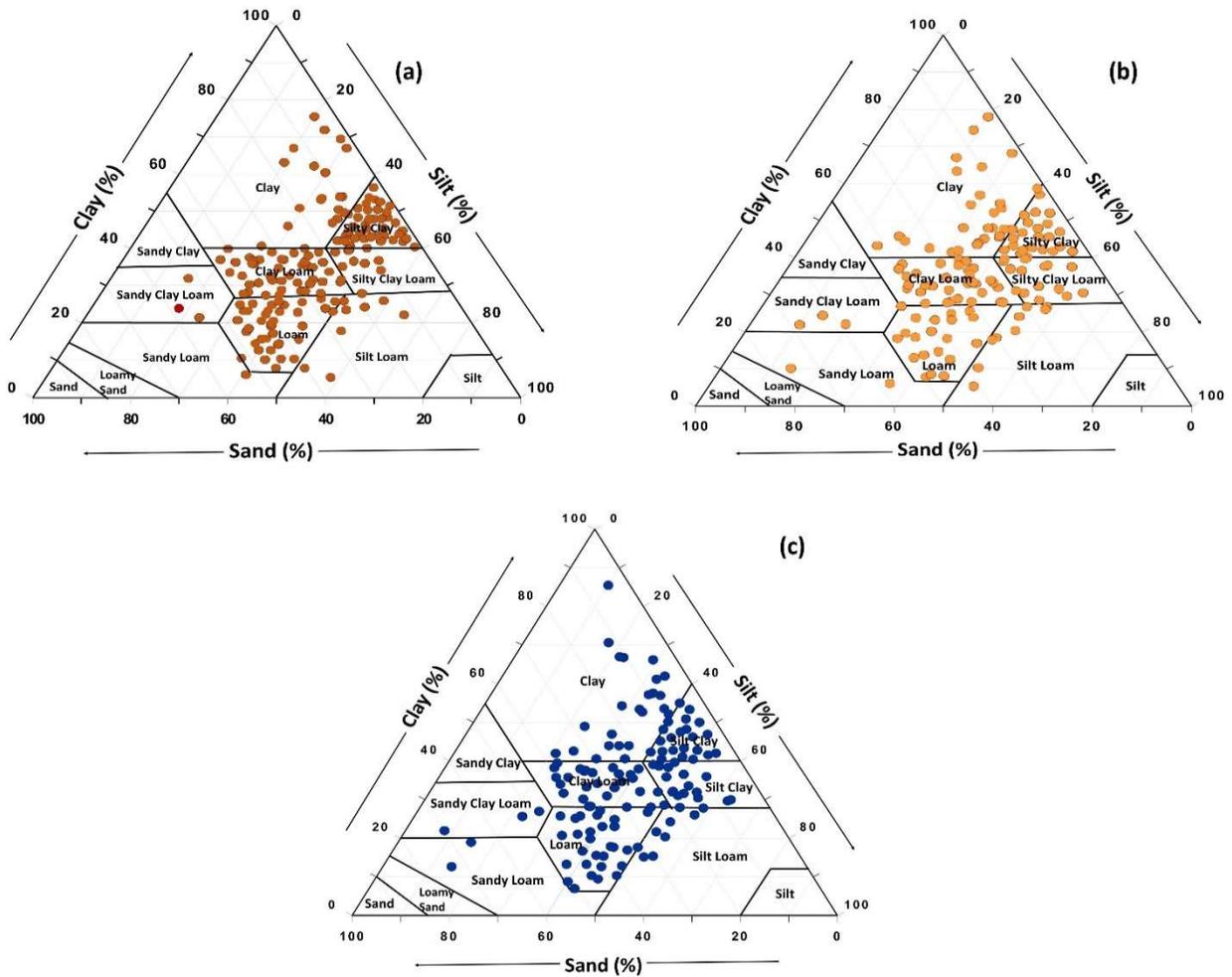
Fig. 3.1: Ternary plots of soil texture in Indus Delta. (a) 0-20 cm, (b) 20-40 cm, and (c) 40-60 cm soil depth

The spatial variations in soil texture of Indus delta at 0-20, 20-40, and 40-60 cm soil depths are presented in Fig. 3.2 (a, b and c), respectively. There is no any specific trend in the spatial variation of texture in the delta. However, coastal areas were dominated with silty clay, silty clay loam, and silt loam classes. The lower soil layers (20-40 and 40-60 cm) had nearly similar soil texture distribution pattern.
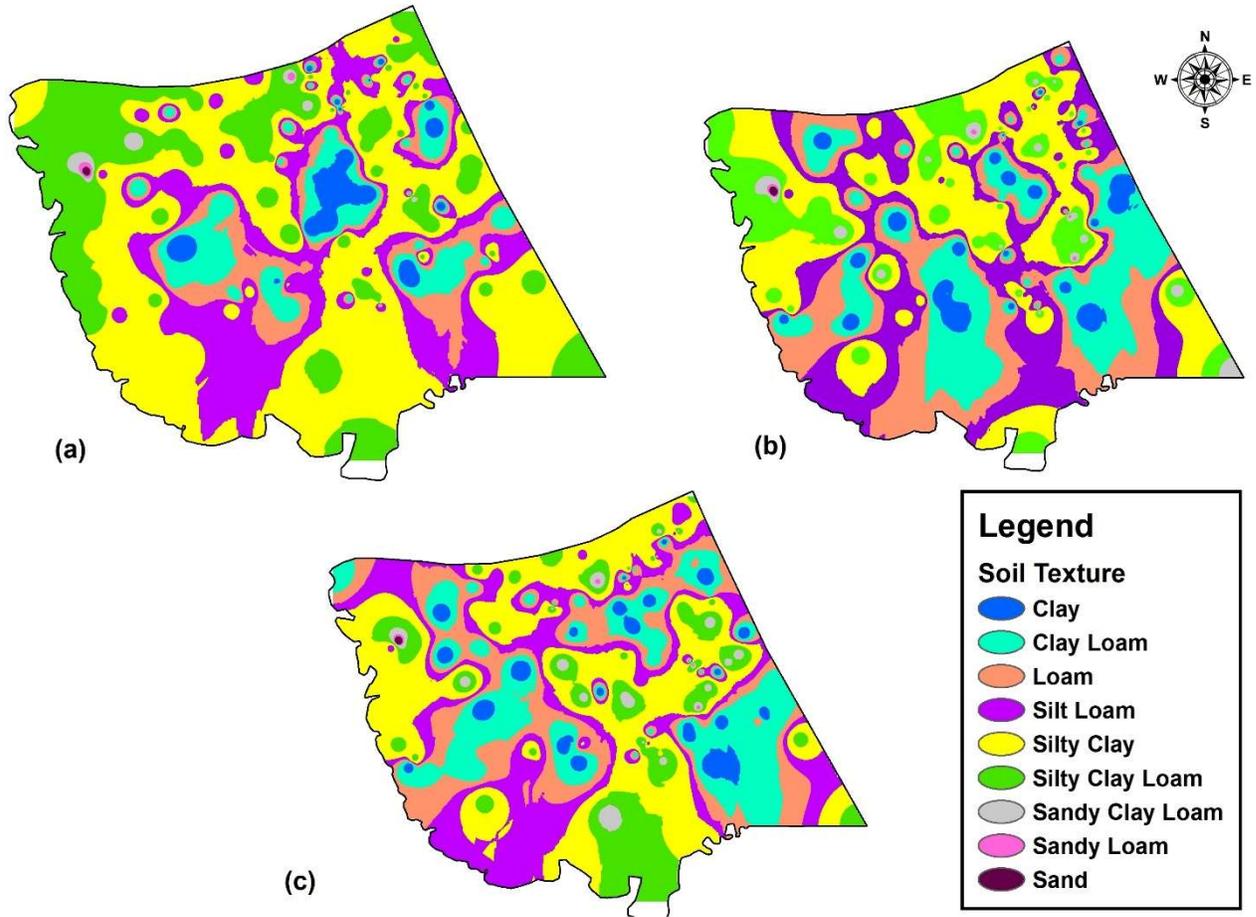
Fig. 3.2: Interpolated maps showing spatial variation in soil texture (a) 0-20 cm, (b) 20-40 cm, and (c) 40-60 cm soil depth

About 48% of soil samples collected from the delta had silty clay and clay loam, 16% had loam, 15% had clay, and 10% had silty clay loam soil texture in the 0-60 soil profile. While silt loam, sandy clay loam, sandy loam, and sand soil textures were found in only 11% of the samples (Fig. 3.3). Thus, the soils of the delta are dominated with heavy fine-textured soils. Similar results are reported by Majeed et al. (2010), who found that most of the soils in the area (>80%) are clay and clay loams. FFC (2005) revealed that particle size distribution of suspended sediment in river Indus

below Kotri on average contains 5.0% sand, 49.6% clay and 45.4% silt; hence the alluvial soils of the delta are dominated with the fine-textured soils
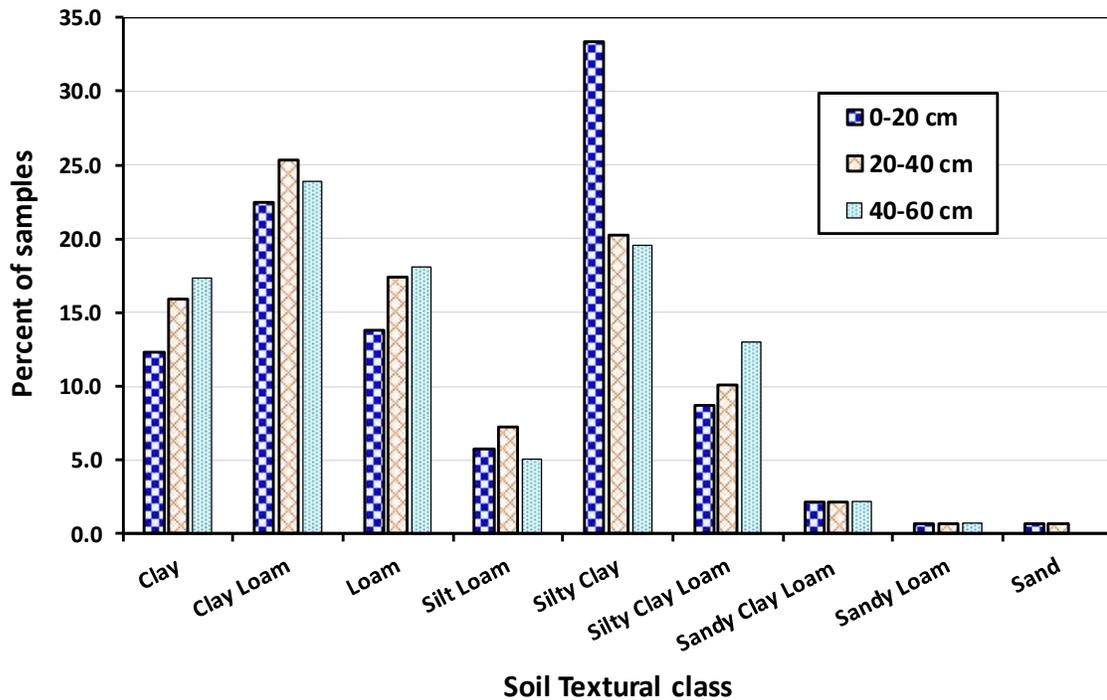
Fig. 3.3: Percentage of soil samples having different soil textural classes

3.1.2   Interpolated EC, pH, ESP and soil salinity

Based on analysis of soil samples collected from the entire Indus delta, the interpolated soil EC maps of all three considered soil depths were prepared and are presented in Fig. 3.4. It shows that vast area located in the south of Delta along the coast have EC greater than 15 dS/m may be due to the impact of subsurface seawater intrusion. EC decreased significantly in areas located away from the sea. There was increasing EC of soil with decreasing soil depth. The higher values of EC in the topsoil are due to the migration of salts from lower soil layers with the capillary movement of water in the top layer where the water evaporates while leaving salts on the surface (Yu et al., 2014). The electrical conductivity of soil at 0-20 cm depth of the Indus delta varied from 0.45 to 55.2 dS/m with an average value of 14.28±2.4 dS/m. The EC of top 0-20 cm layer of 12.1% of delta (or 23.8% of Delta if tidal flood area is not included) was below 4 dS/m. While EC was less than 4 dS/m in 20-40 cm and 40-60 cm soil depths in 15.2% (or 30.12%) and 19.7 (or 38.9%) of the delta respectively.
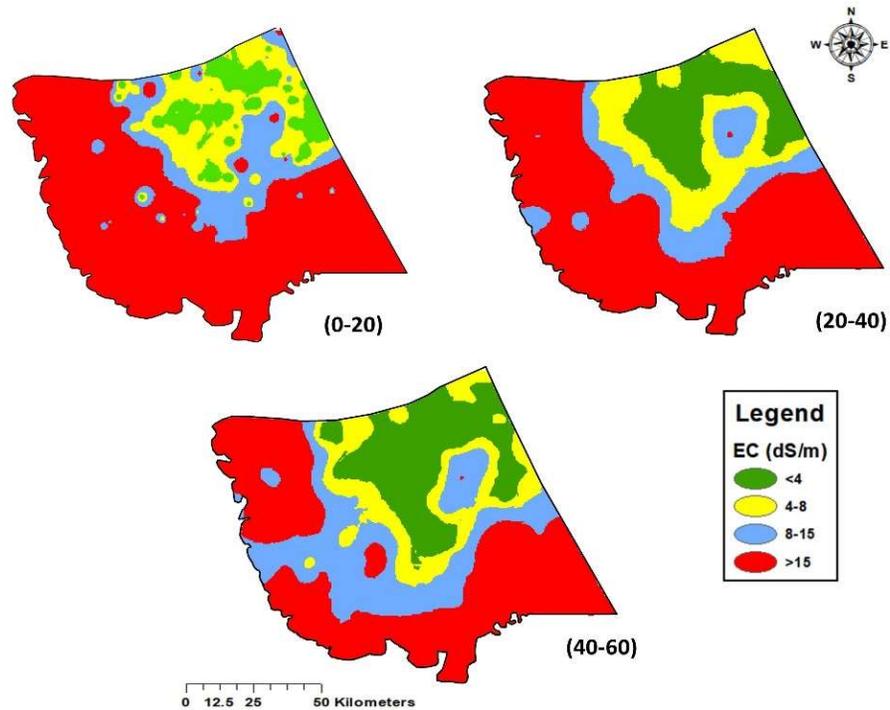
Fig. 3.4: Interpolated maps of Electrical Conductivity of soil saturation extract (EC) of Indus delta at 0-20, 20-40 and 40-60 cm soil depths

The pH of soil saturation extract of soil samples collected from 0-20 cm soil depth varied between 7.7 to 11.4 with a mean value of 8.9, whereas, the pH of soil at 20-40 cm soil depth varied from 7.1 to 9.2 with an average value of 7.9. However, the pH in 40-60 cm soil depth ranged between 7.2 and 9.2, with an average value of 8.0. Generally, the soils having a pH value higher than 8.5 are considered as sodic soils. A soil having a pH of 7.0 is neutral, below 7.0 indicates increasing acidity. The values of pH above 7.0 to a maximum of 14.0, indicates increasing alkalinity. In the study area, most of the sampled soil had pH values within the range of 8.5. However, the pH values of soil samples collected from and nearby tidal floodplains had higher values of pH, might be due to higher sodium content in the soils. The spatial distribution of the soil pH in the study area is portrayed through interpolated GIS maps in Fig. 3.5.
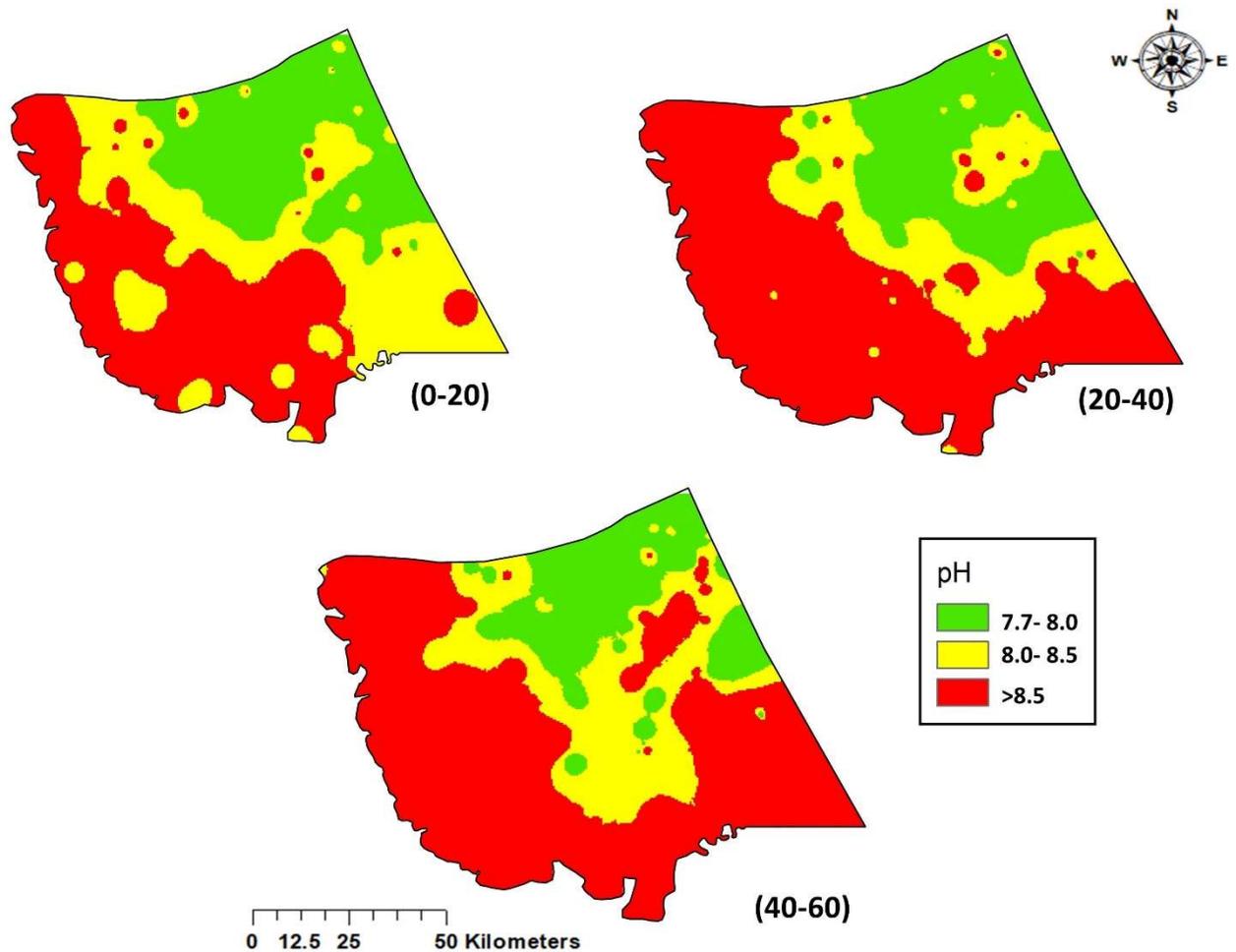
Fig. 3.5: Interpolated maps of soil pH of Indus delta at 0-20, 20-40 and 40-60 cm soil depths

ESP of 0-20 cm soil depth of the Indus delta ranged from 1.4 to 65.6 with an average of 25.2±2.6. The soils having ESP value greater than 15 is classified as sodic or saline-sodic soils. In this regard, about 72.8% of the soil samples had ESP values greater than the threshold level of 15. In 20-40 cm soil depth, the ESP values ranged from 5.2 to 66.5, with an average of 26.6±2.6. However, about 72.0% of the soil samples of the 20-40 cm layer had ESP values greater than the safe limit. The ESP values of 40-60 cm soil depth ranged from 3.6 to 65.8, with an average value of 27.06±2.5. About 79.2% of the sampled soil of the last layer had ESP values greater than the threshold value of 15. Fig. 3.6 represents the spatial distribution of ESP for 0- 20, 20-40, and 40-60 cm soil depths of the Indus Delta.
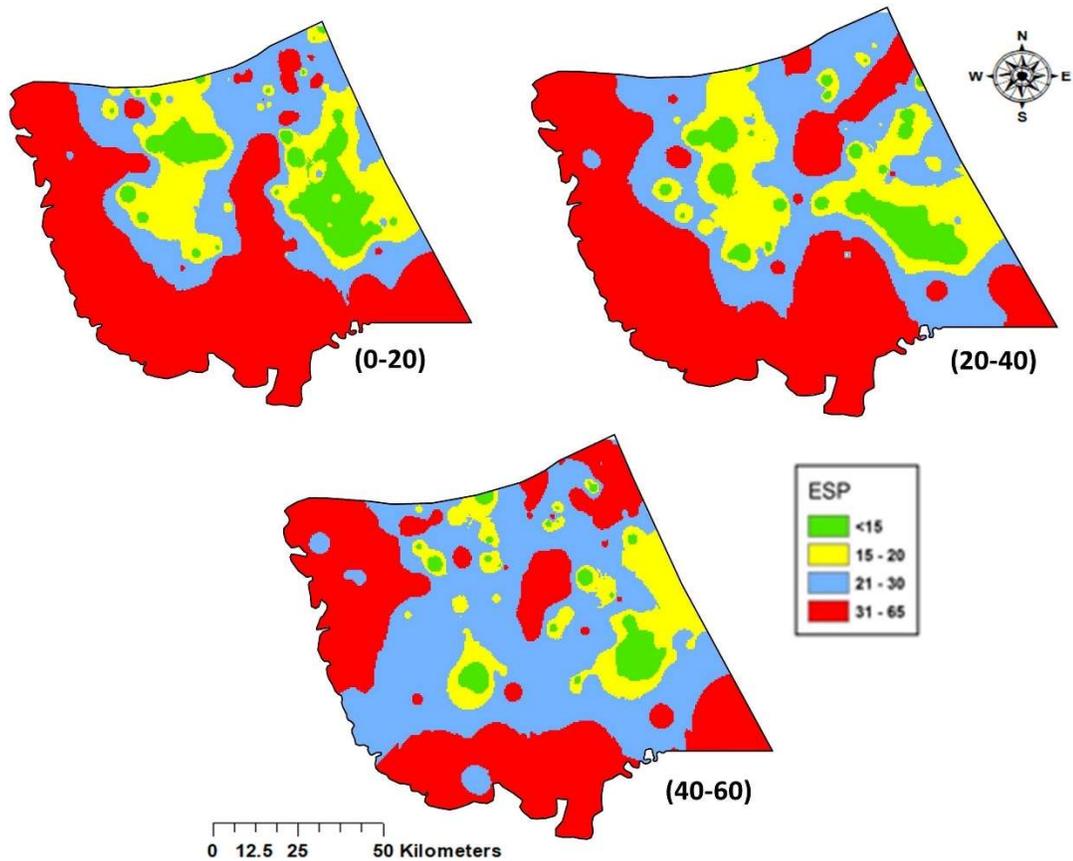
Fig. 3.6: Interpolated maps of soil ESP of Indus delta at 0-20, 20-40 and 40-60 cm soil depths

Based on ground truthing field data and analysis of soil samples, spatial distribution thematic maps for soil salinity, i.e., normal, saline, sodic, and saline-sodic for all the three soil depths viz. 0-20 cm, 20-40 cm, and 40-60 cm were prepared (Fig. 3.7).

The interpolated spatial distribution soil salinity maps showed that more than 80% of the Indus delta was salt-affected. There was a higher level of salinity in those samples which were taken from the tidal floodplains of the delta adjacent to the Arabian Sea, which might be due to surface and subsurface seawater intrusion. It was also revealed that the salinity in the topsoil was higher than that in subsoil indicating that the salts in the subsoil move up and accumulate in the topsoil.
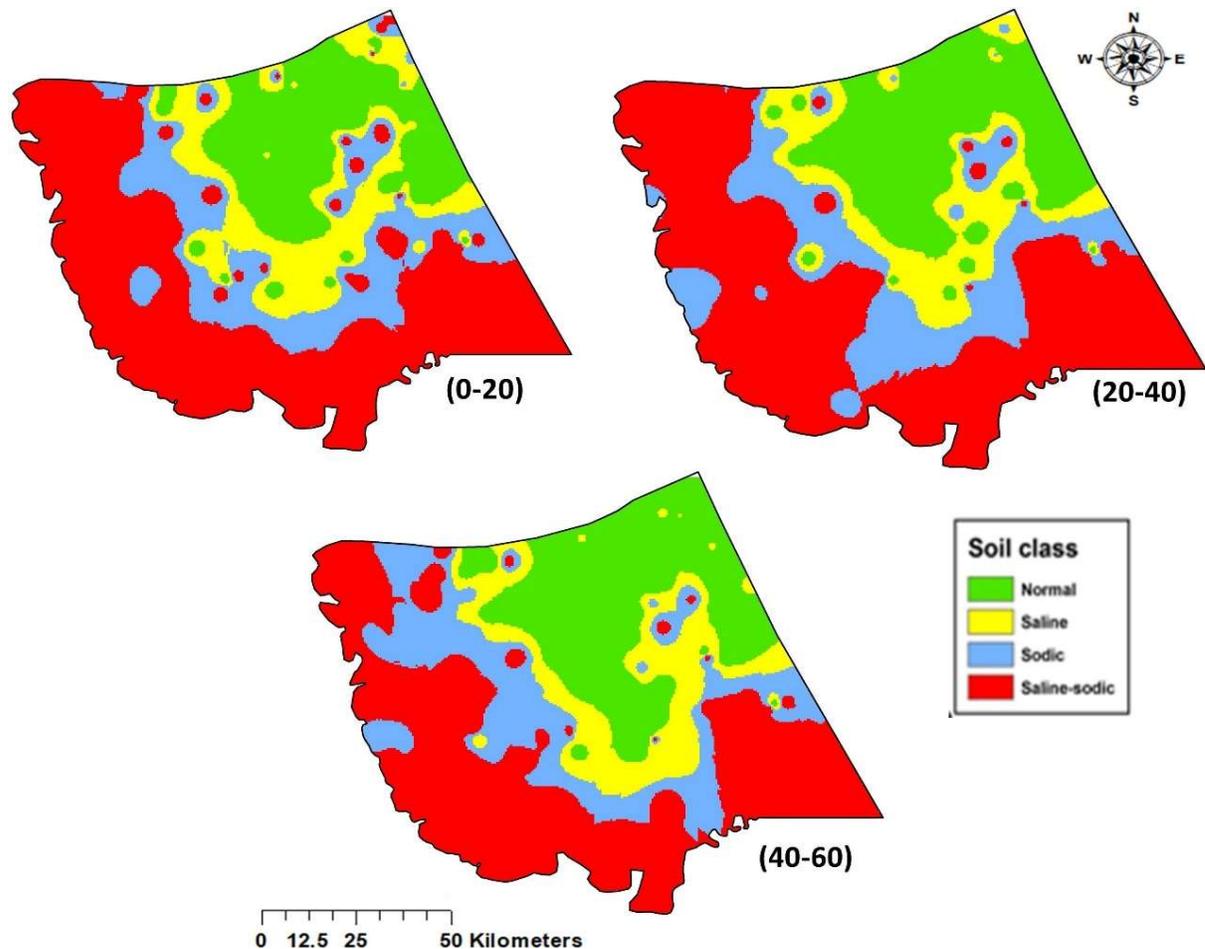
Fig. 3.7: Interpolated maps of soil salinity classification of Indus delta at 0-20, 20-40 and 40-60 cm soil depths

3.1.3   Temporal change in soil salinity using satellite data

Fig. 3.8 shows the maps of temporal and special change in the soil salinity of Indus delta during the last 30 years, i.e., from 1990 to 2019. The classified maps based on the soil salinity indices show that the vast areas of land are salt-affected between the tidal floodplain areas and the irrigated areas. The high soil salinity in these areas might be due to the result of the unavailability of irrigation water at the tail end of the canal system to leach down the salts. Moreover, subsurface seawater intrusion is the main reason of soil salinity in these areas. Based on classified images, the land use of the Indus delta is quantified in Table 3.1. It shows that salt affected irrigated land increased from 57.4% to 57.7% of the delta during the last three decades. Whereas, the area under normal soil decreased from 29.3% of the delta to 26.7% during the last 30 years. It reflects that

with the passage of time, the normal productive soil is converting into unproductive salt affected the soil in the delta.
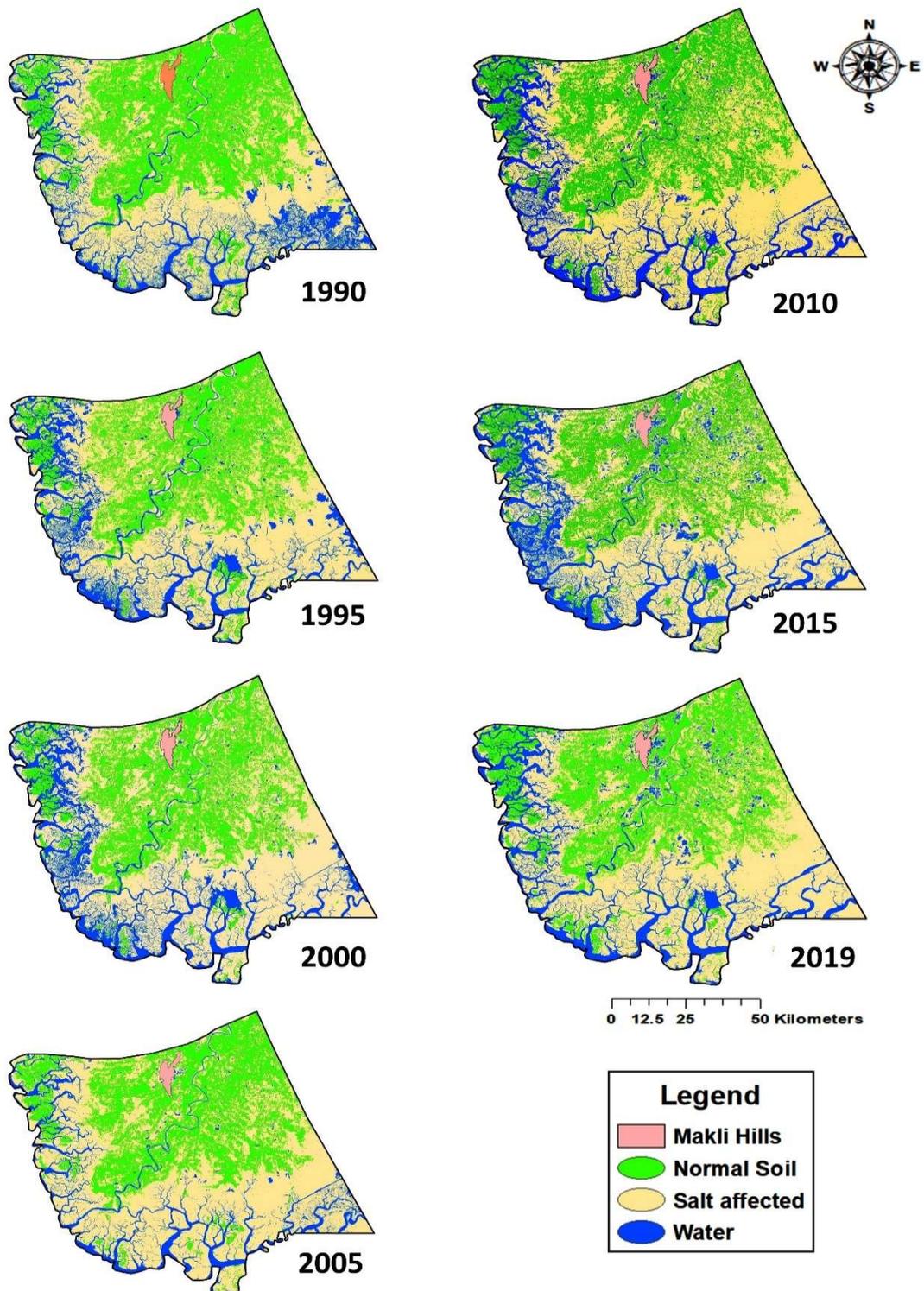
Fig. 3.8: Classified satellite images of Indus Delta showing the temporal and spatial variation in the soil salinity

Table 3.1   Land use of Indus delta based on classified satellite images.

Year	Water		Normal/Vegegtation		Salt affected		Makli Hills	
	sq. km	% of delta	sq. km	% of delta	sq. km	% of delta	sq. km	% of delta
1990	2009.377	15.38	3825.395	29.28	7150	54.72	82.7	0.63
1995	2051.846	15.70	3667.554	28.07	7265.074	55.60	82.7	0.63
2000	2059.297	15.76	3531.149	27.02	7394.027	56.59	82.7	0.63
2005	1780.151	13.62	3317.589	25.39	7886.049	60.35	82.7	0.63
2010	1990.4	15.23	3360.605	25.72	7633.471	58.42	82.7	0.63
2015	2180.038	16.68	3397.316	26.00	7407.42	56.69	82.7	0.63
2019	1949.549	14.92	3491.844	26.72	7542.698	57.72	82.7	0.63

The temporal variation in salt-affected soils of Indus delta from 1990 to 2019 was quantified from the satellite imagery of Landsat satellites and is presented in Table 3.2. The salt affected area and area under water and towns/cities were 70% of delta in 1990, which increased to 73% of the delta after 29 years in 2019. While through interpolation, salt-affected area and area under water and towns/cities were determined as 76% of the Indus delta.

Table 3.2   Salt-affected area of the Indus delta based on interpolation and satellite imagery

Soil Type	Interpolation	Satellite data
	% of delta	% of delta
1990		
Normal	*	30
Salt affected land and water + built up areas	*	70
2019		
Normal	24	27
Salt affected land and water + built up areas	76	73

24

3.2 Developing a linkage/relation of the current soil salinity profiles (observed spatially and vertically using state of the art field equipment/instruments) with the changes in freshwater supplies downstream of Kotri

The impact of anthropogenic activities on the Indus delta is reflected through the reduced water, and sediment flows below the Kotri Barrage. Fig. 3.9 shows the total volume of water in the river Indus, reaching to sea from the year 1937-38 to 2018. It reflects that with the passage of time the availability of river Indus water decreased linearly especially after the construction of the Guddu barrage in 1955, Mangla Dam in 1967, and Tarbela dam in 1976 (Gupta, 2008). As a result, there is a decrease of about 90 to 400 million tons per year in incoming sediment to delta (Aziz and Khan, 2001; Amjad et al., 2007). It is reported that dams and reservoirs constructed on rivers have barred 20% of the global sediment from reaching the delta (Syvitski et al., 2005). For Indus, the situation is more serious. Before the construction of dams and barrages over the Indus River system, the recorded average annual discharge of water and sediment below Kotri Barrage was 107 billion cubic meters (BCM) and 193 million tons, respectively (Gupta, 2008). From the year 1998 to date, water, and sediment discharges have decreased at an alarming rate below Kotri Barrage, except the years 2010 and 2014.
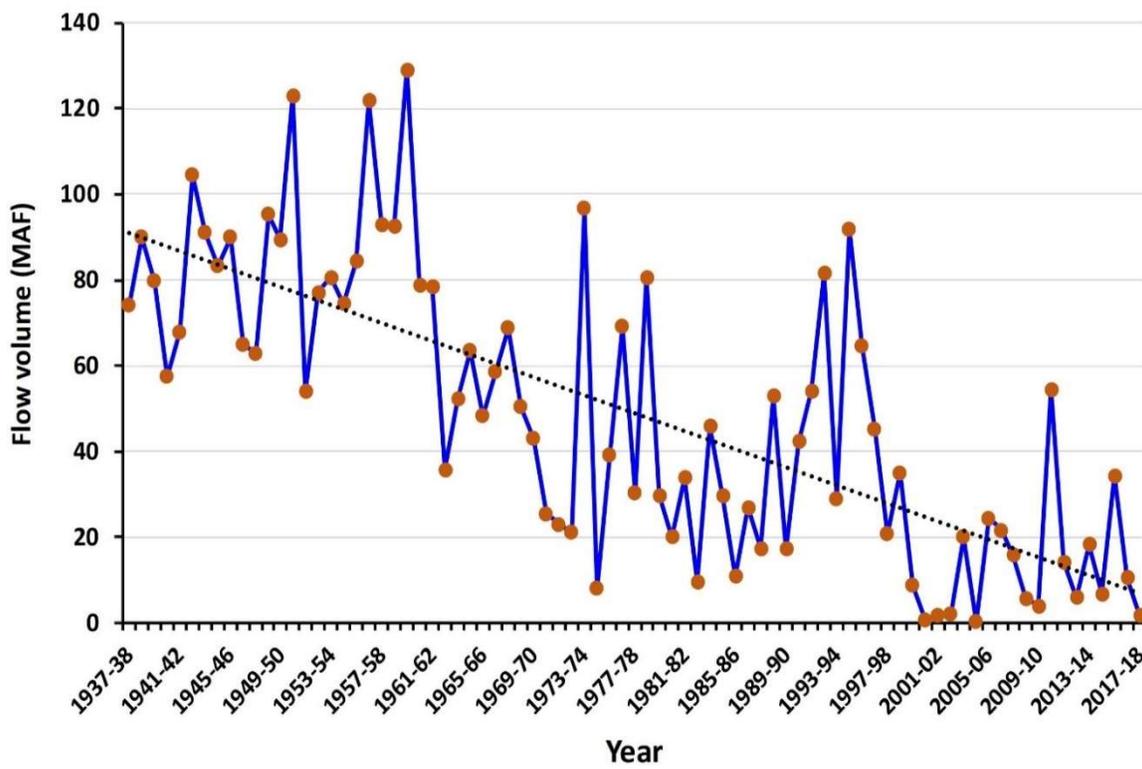
Fig. 3.9: Temporal change in the river Indus river flow below Kotri barrage

To get a clear picture about the decreased flow to delta, yearly flow below Kotri downstream for the last two decades is plotted in Fig. 3.10. It reflects that out of eighteen years, in half of the years, Indus delta even could not get its minimum requirement of water, i.e. 9.8 million-acre feet (MAF), as suggested by the International Panel of Experts (IPOE) in 2004.
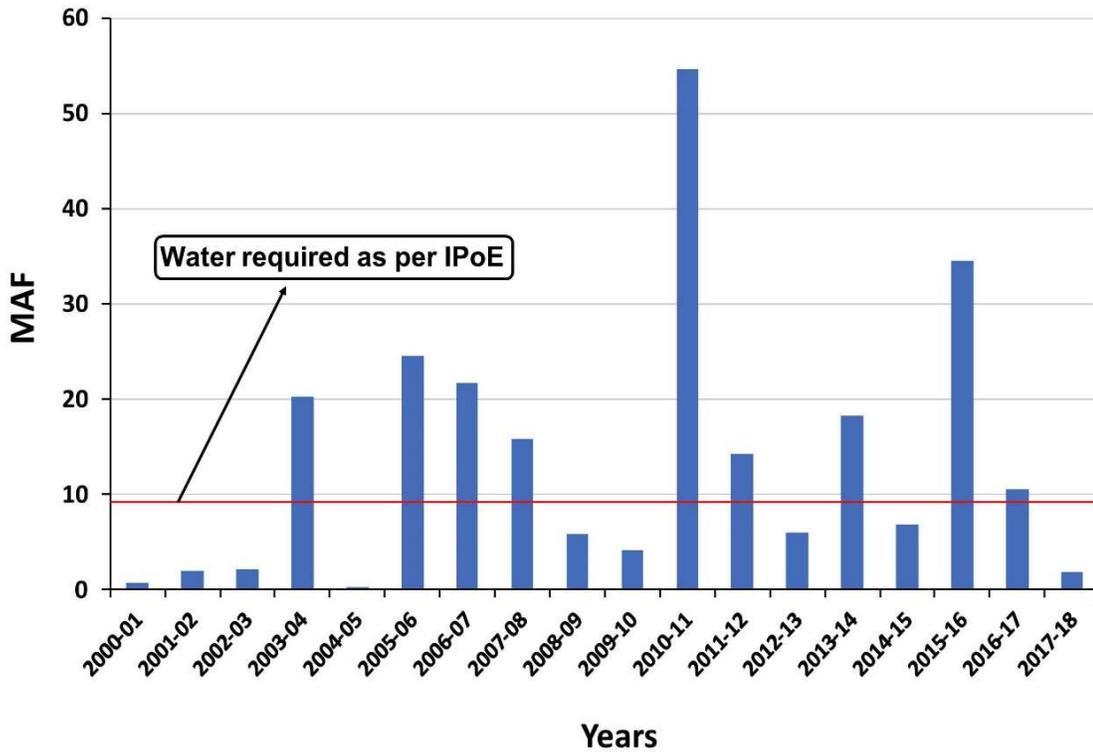
Fig. 3.10: Water released below Kotri barrage from 2001 to 2018 and the environmental river flow recommended by IPOE

The impact of the construction of hydraulic structures on the Indus River water flow can be judged from the number of days with no flow below Kotri Barrage. Until 1962, there was not a single day with zero flow before Kotri Barrage (Fig. 3.11). Zero-flow days started after commissioning of Kotri and Guddu Barrages during 1962-1967; the maximum number of days in a year increased to 100. Days with no or zero flow increased up to 250 days during the post-Kotri and post-Mangla period (1967–1975). Currently, downstream Kotri Barrage flow is constrained mainly in only two months of monsoon, i.e., August-September (Gupta, 2008). As a result, sediment passing below the Kotri barrage tends to be deposited in the river bed near Kotri barrage rather than reaching to sea and maintaining the growth of the delta. Thus, sand bars are developed in the river bed immediately after the Kotri barrage.
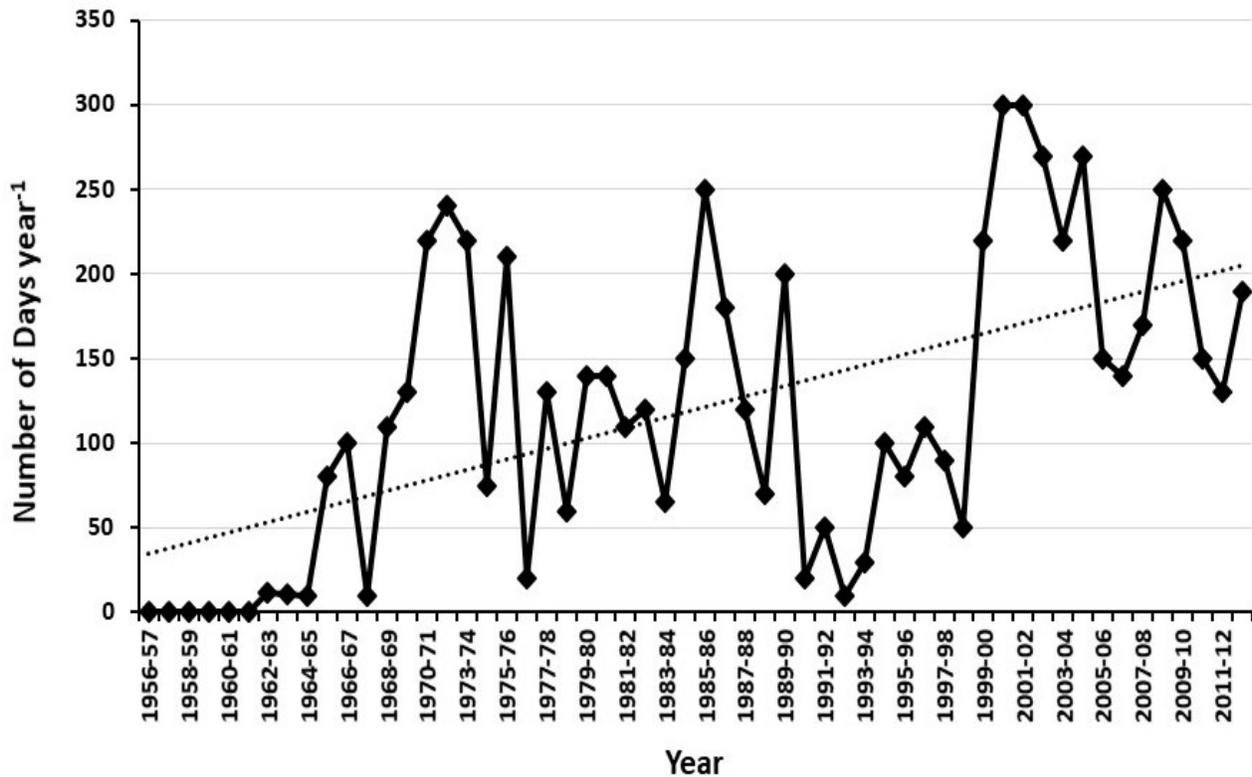
Fig. 3.11: Zero or no flow days per year below Kotri barrage

In order to determine the impact of between Kotri downstream flow and the salt-affected area in the Indus delta, the volume of water released in five years was plotted against the corresponding area under salt affect soils after every five years as shown in Fig. 3.12. It depicts that there is a negative and weak relation between the volume of water released and the area under salt affected soils with a coefficient of determination of $R^2 = 0.483$. This suggests that the decrease in river flow below Kotri has an impact of 45% on the development of soil salinity. The other factors contributing to the development of the soil salinity in Indus delta might be the subsurface seawater intrusion, low rainfall, and increase in temperature under changing climate scenario. Thus, increased river-flows, supplemented by required environmental river-flows, can be helpful in mitigating soil salinity issue in deltaic areas (Salik, 2016). However, for addressing the soil salinity issue in delta, it will be supportive of providing sufficient water for irrigation up to tail end through canal network present the delta.
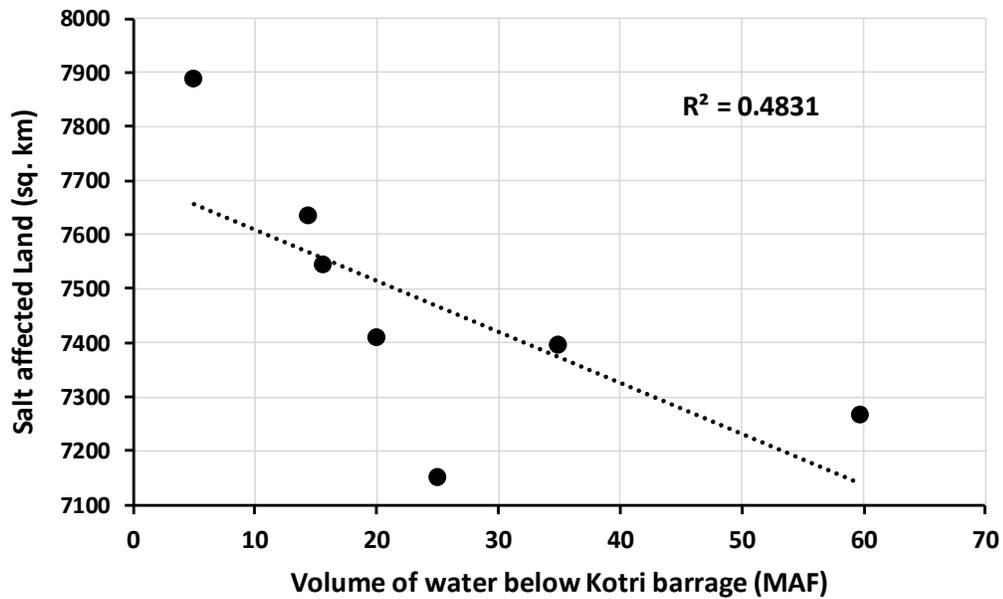
Fig. 3.12: Relationship between the salt-affected area and the volume of water released below Kotri barrage in five years

Fig. 3.13 shows the relation between Kotri downstream flow and the normal soil area. It depicts a weak but positive relation with a coefficient of determination of $R^2 = 0.37$ between the two variables. It reflects that with an increase in flow below Kotri downstream, there is a slight increase in the normal soil and decrease in soil salinity. It might be due to the leaching of salts from the soil surface due to the application of irrigation water from crop growth.
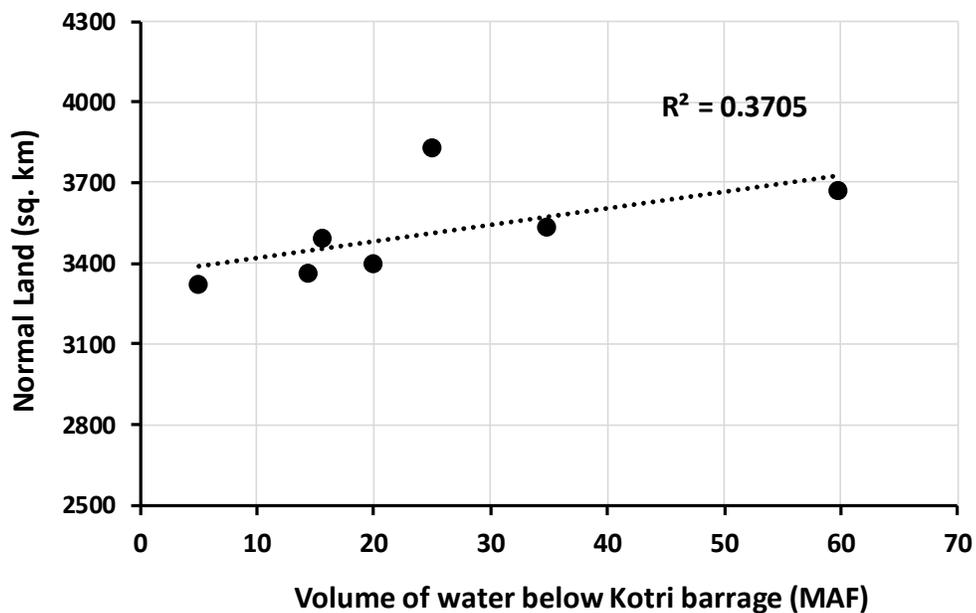
Fig. 3.13: Relationship between area under normal soil and the volume of water released below Kotri barrage in five years

28

3.3 Coastal area inundation under different sea level rise scenarios and estimation of associated environmental/economic loss.

The rise in average sea level amplifies the impacts of extreme events on coastal environment, geomorphology, and landscape. Depending upon coastal topography, and the existence of protective infrastructure such as levees, and dikes, a small increase in the average sea level can have drastic impacts on the inland extent and frequency of flooding events (Kirshen et al., 2008). The thematic map of the variation in elevation of the entire delta is presented in Fig. 3.14. The Figure shows that the lowest elevation of delta (0-3 m) is along the seacoast while Makli hills have the highest elevation, which ranges between 20 to 60 m. McGranahan et al. (2007) and Lichter et al. (2011) defined low-elevation coastal zone (LECZ) as the contiguous and hydrologically connected zone of land along the coast and having an elevation below 10 m. Thus, the Figure shows that vast areas of the delta can be categorized as LECZ.
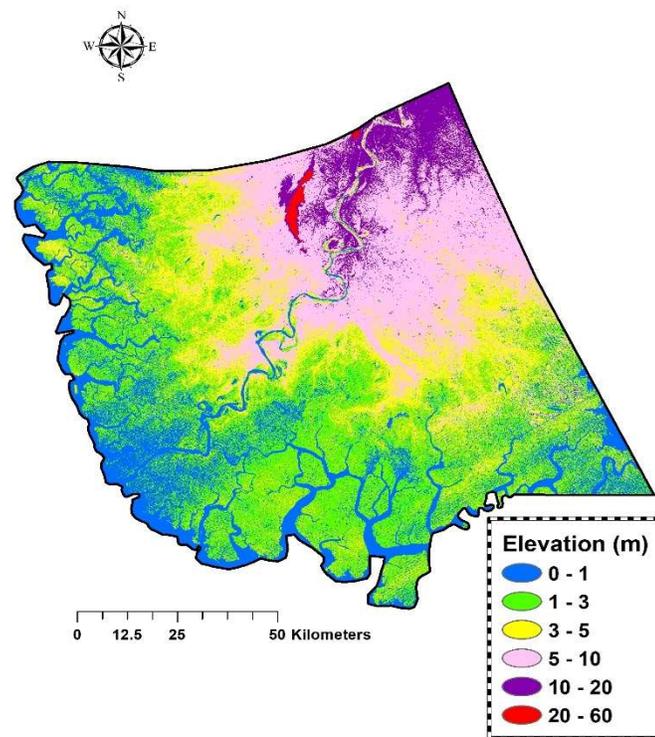
Fig 3.14 Thematic map of the variation in elevation of the entire delta

The analysis of the DEM revealed that about 29400 sq. km area or 22.5% of the delta has an elevation of less than 1 m. About 69% of the delta or 90410 sq. km of the land surface has an elevation of less than 5m above mean sea level (MSL) as shown in the graph (Fig.3.15). The area

of Indus delta under LECZ is about 12248 sq. km or 93.7% of the delta which mimics the severity of the problem of coastal inundation.
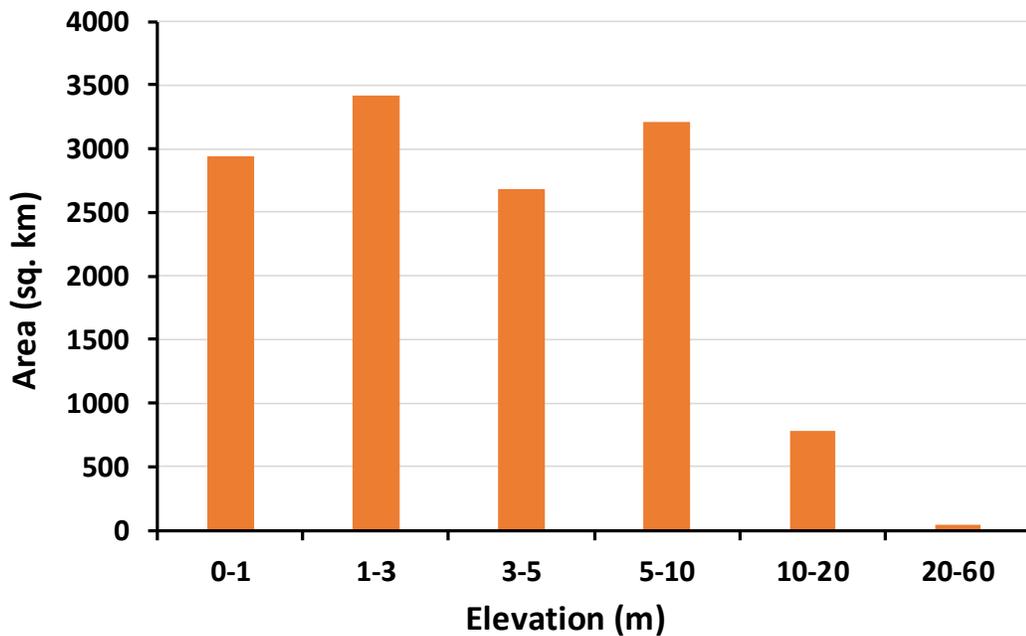
Fig 3.15 Areas of Indus delta at different elevations above mean sea level (MSL)

Fig 3.16 shows the flood risk map of the Indus delta. It reflects that about 94% of the delta or 12250 sq. km falls in the LECZ; thus, highly vulnerable to coastal inundation. Almost, all major cities of the delta are located in LECZ, hence are under high risk of coastal flood inundation.
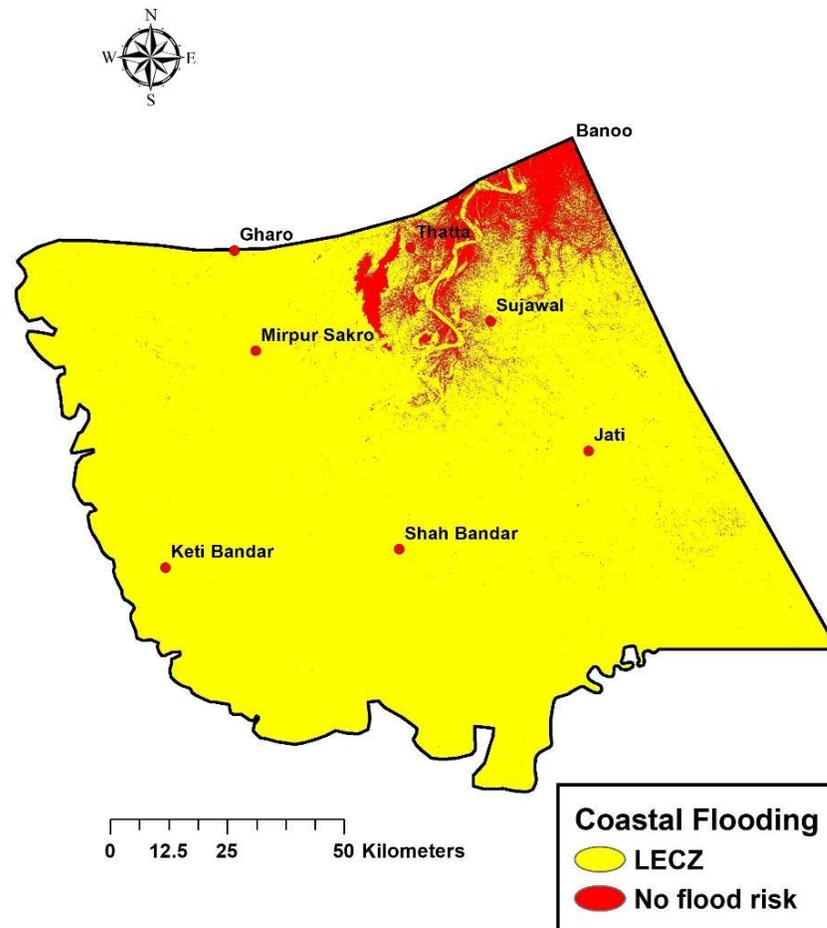
Fig. 3.16 Flood risk map of Indus Delta

3.3.1 *Estimation of associated environmental/economic loss*

The degradation, shrinking, and coastal flooding of Indus delta has a significant impact on the environment and the economic conditions of the delta. World Bank (2019) estimated the economic cost of degradation of the Indus Delta around US$2 billion annually. The costs of pollution and other environmental degradation was not assessed. Sanchez-Triana et al. (2015) reported that in the delta about half is agricultural loss due to waterlogging and salinity while half loss of delta is the degradation of the ecosystem, including mangrove forests and fisheries.

From Table 3.2, about 24% of delta (313608 ha) is cultivable agricultural land, and out of which suppose 70% (219500 ha or 542450 acres) is actually cultivated during Rabi and Kharif seasons. Since 93% of delta falls within LECZ, hence due to coastal flooding, about 504450 acres of land are estimated vulnerable for flooding. If average rice crop yield is 60 Maunds per acre and price per maund is Rs. 1000 then the agricultural economic loss of delta due to coastal flooding in Kharif season could be estimated as Rs. 30 billion. Similarly, If the coastal flooding occurs during Rabi

31

season, the agricultural loss could be estimated as Rs. 27 billion. Except for agricultural loss, environmental, ecological and infrastructure losses would also be severe.

4.   CONCLUSIONS

Based on ground truthing of the Indus delta, EMI survey, analysis of soil samples, secondary data, and temporal satellite imagery, the following conclusions are drawn from the present study:

- About 48% of soil samples had silty clay and clay loam, 16% had loam, 15% had clay, and 10% had silty clay loam soil texture in the 0-60 soil profile. While silt loam, sandy clay loam, sandy loam, and sand soil textures were found in only 11% of the samples. It reflects that for all depths, the majority of soil textures had silty clay, clay loam, and loam textural classes. Thus, the soils of the delta are dominated with heavy fine-textured soils.

- The vast areas in the south of Delta along the coast have EC greater than 15 dS/m, may be due to the impact of subsurface seawater intrusion. EC decreased significantly in areas located away from the sea. There was increasing EC of soil with decreasing soil depth.

- Most of the sampled soil had pH values within 8.5. However, the pH values of soil samples collected from and nearby tidal floodplains had higher values of pH, might be due to higher sodium content in the soils.

- The interpolated soil salinity maps showed that more than 80% of the soils in Indus delta were salt-affected.

- The salt affected irrigated land increased from 57.4% to 57.7% of the delta during the last three decades. Whereas, the area under normal soil decreased from 29.3% of the delta to 26.7% during the same period.

- Before the construction of dams and barrages over the Indus River system, the average annual discharge of water and sediment below Kotri Barrage was 107 billion cubic meters (BCM) and 193 million tons, respectively which has decreased significantly especially after the year 2000.

- Until 1962, there was not a single day with zero flow before Kotri Barrage. Zero-flow days started after commissioning of Kotri and Guddu Barrages during 1962-1967. Currently, downstream Kotri Barrage flow is constrained mainly in only two months of monsoon, i.e., August-September

- The volume of water released in five years plotted against the corresponding area under salt affect soils after every five years depicted that there was a negative and weak relation between the volume of water released and the area under salt affected soils with a coefficient of determination of $R^2 = 0.483$.

- A weak but positive relationship with a coefficient of determination of $R^2 = 0.37$ between the Kotri downstream flow and the normal soil area was observed. It reflects that with an increase in flow below Kotri downstream, there is a slight increase in the normal soil and thus decrease in soil salinity.

- A low-elevation coastal zone (LECZ) having an elevation below 10 m spreads over vast areas of the delta. Analysis of DEM portrays that about 94% of the delta or 12250 sq. km of delta fall within the LECZ; thus, highly vulnerable to coastal inundation. Almost, all major cities of the delta are located in LECZ, hence are under high risk of coastal flood inundation.

- The degradation, shrinking, and coastal flooding of Indus delta has a significant impact on the environment and the economic conditions of the delta. It is estimated the economic cost of degradation of the Indus Delta around US$2 billion annually. The costs of pollution and other environmental degradation was not assessed.

- About 24% of delta (313608 ha) is cultivable agricultural land, and out of which suppose 70% (219500 ha or 542450 acres) is actually cultivated during Rabi and Kharif seasons. Since 93% of delta falls within LECZ, hence due to coastal flooding, about 504450 acres of land will be submerged. If average rice crop yield is 60 Maunds per acre and price per maund is Rs. 1000, then the agricultural economic loss of delta due to coastal flooding in Kharif season could be estimated as Rs. 30 billion. Similarly, If the coastal flooding occurs during Rabi season, the agricultural loss could be estimated as Rs. 27 billion. Except for agricultural loss, environmental, ecological and infrastructure losses would also be severe.

5. RECOMMENDATIONS

Based on the present study, the following are the recommendations for the policymakers for mitigation of the adverse impacts of seawater intrusion in the Indus delta under changing climate scenario:

- Biosaline agriculture should be introduced and encouraged by the government in tidal floodplains and over the vast barren salt-affected soils lying between tidal floodplains and the canal irrigated areas of the delta especially on the left bank of river Indus. Pal grass, Quinoa, Salicornia, Sea Aster, Spartina alterniflora, etc. have a bright scope of cultivation and high yield in these areas. Biosaline agriculture will certainly be a source of food and fodder for the coastal communities and livestock. Thus, it will help in the mitigation of poverty and in improving the coastal environment under changing climate scenario.

- A 38 km long coastal highway constructed at the periphery of the tidal floodplain on the right bank of Indus should be extended 180 km further on the left bank of Indus by putting a bridge over the river Indus at Kharo Chhan. The proposed highway will not only provide coastal communities with quick and easy access to the markets of Karachi but will also attract the tourists and flourish tourism in the delta. Hence, socio-economic conditions of poor communities of the delta will be improved. Also, it will act as a defense-line against the surface seawater intrusion, thus will impede further swallowing of the delta by sea. It will also act as a barrier against coastal flooding due to tsunami, cyclone, or any other natural disaster.

- As per recommendations of International Experts (IPOE) in 2004; water flow of 5000 cusecs throughout the year should be ensured below Kotri Barrage to minimize the impact of seawater intrusion and meet the environmental flow needs flora and fauna. Also, a total volume of 25 MAF in five years (equivalent to 5 MAF annually) be released below Kotri barrage as flood flows (Kharif period).

- For minimizing surface and subsurface seawater intrusion in the entire delta, sufficient water in canals originating from Kotri Barrage should be ensured along with the environmental flow in the river. It will not only minimize seawater intrusion but also provide drinking water to coastal communities and mitigate adverse impacts on the ecosystem of the delta. Satellite images provide evidence that irrigation channels of the delta have a significant impact on the seawater intrusion in areas far from the river Indus.

- If possible, old relic river channels, such as Ochito and Old Pinyari, should be restored. These channels, if restored, will carry extra flood water to the sea during a high flood and thus shun the pressure on the levees of the main river and thus minimize the possibility of the levee breach. It will also supply fresh water to the coastal communities living far away from the main river course.

- Most of the natural lakes in the delta are saline, which should be revitalized by adding freshwater during the monsoon period. Freshwater lakes can play a vital role in providing drinking water to the communities and also work as groundwater recharge hotspots.

- Tourism Industry should be encouraged, especially boat cruising in the mangrove laden creeks in the Delta to improve socioeconomic conditions of poor local communities.

6. References

Ahmed, W., and Shaukat, S. S. (2015). Status of mangroves of north-western part of Indus delta: environmental characteristics and population structure. Pakistan Journal of Marine Sciences, 24(1&2): 61-85.

Amanullah, M.; Ahmed, A.; & Ali, G. (2014). Ecological impacts of altered environmental flow on Indus Deltaic ecosystem, Pakistan: a review. Journal of Environmental Professionals Sri Lanka, 3(1): 11-21.

Asfaw, E.; Suryabhagavan, K. V., & Argaw, M. (2018). Soil salinity modeling and mapping using remote sensing and GIS: the case of Wonji sugar cane irrigation farm, Ethiopia. Journal of the Saudi Society of Agricultural Sciences, 17(3), 250-258.

Amjad, A.S.; Kasawani, I.; Kamar-u-zaman, J. (2007). Degradation of Indus delta mangroves in Pakistan. Int. J. Geol. 3, 27–34.

Aziz, I., & Khan, M. A. (2001). Experimental assessment of salinity tolerance of Ceriops tagal seedlings and saplings from the Indus delta, Pakistan. Aquatic Botany, 70(3), 259-268.

Baig, M. A.; Sultan, M.; Khan, M. R.; Zhang, L.; Kozlova, M.; Malik, N. A., & Wang, S. (2017). Wetland Change Detection in Protected and Unprotected Indus Coastal and Inland Delta. The International Archives of Photogrammetry, Remote Sensing and Spatial Information Sciences, 42, 1495.

Bouyoucos, G.J. (1936). Directions for Making Mechanical Analysis of Soils by the Hydrometer Method.Soil Science 4:225 – 228.

Callaghan, L., (2014). Working together to protect the Indus River Delta. https://www.koreannewsletter.org/uploads/7/0/4/0/7040474/working_together_to_protect_the_indus_river_delta_liam_o'callaghan.pdf (visited on March 10, 2019).

Chander, G., Markham, B. L., & Helder, D. L. (2009). Summary of current radiometric calibration coefficients for Landsat MSS, TM, ETM+, and EO-1 ALI sensors. Remote sensing of environment, 113(5), 893-903.

Church, J. A., and White, N. J. (2011). Sea-level rise from the late 19th to the early 21st century. Surveys in geophysics, 32(4-5), 585-602.

Corwin, D. L. (2008). Past, present, and future trends in soil electrical conductivity measurements using geophysical methods. In: Allred, B.J., Daniels, J.J., Ehsani, M.R. (Eds.), Handbook of Agricultural Geophysics. CRC Press, Taylor and Francis Group, Boca Raton, Florida, pp. 17–44.

DasGupta, R. and Shaw, R. (2013). Cumulative impacts of human interventions and climate change on Mangrove ecosystems of South and Southeast Asia: An overview. J. Ecosyst. 2013, 1-15.

Doolittle, J. A., & Brevik, E. C. (2014). The use of electromagnetic induction techniques in soils studies. Geoderma, 223, 33-45.

FFC (2005). Study on Water Escapages below Kotri Barrage to check seawater intrusion. (Study-I). Final Report. Ministry of Water and Power. Government of Pakistan

Gee, W.G., and D. Or. 2002. Particle-Size Analysis. In: Dane, J., and G.C. Topp (eds.). Methods of Soil Analysis. Book Series: 5. Part 4. Soil Science Society of America. USA. p. 255–293.

Ghabour, T.K. and Daels, L. (1993). Mapping and monitoring of soil salinity of ISSN. Egyptian Journal of Soil Science 33: (4)355-370.

Gupta, A. (Ed.). (2008). Large rivers: geomorphology and management. John Wiley & Sons.

Douaoui, A. E. K.; Nicolas, H. and Walter, C. (2006). Detecting salinity hazards within a semiarid context by means of combining soil and remote-sensing data. Geoderma 134(1), 217-230.

Giosan, L.; Syvitski, J.; Constantinescu, S., and Day, J. (2014). Climate change: protect the world's deltas. Nature, 516, 31–33.doi:10.1038/516031a

Giosan, L.; Constantinescu, S.; Clift, P. D.; Tabrez, A. R.; Danish, M., & Inam, A. (2006). Recent morpho-dynamics of the Indus delta shore and shelf. Continental Shelf Research, 26(14), 1668-1684.

Giri, C.; Long, J.; Abbas, S.; Murali, R. M.; Qamer, F. M.; Pengra, B., & Thau, D. (2015). Distribution and dynamics of mangrove forests of South Asia. Journal of Environmental Management, 148: 101-111.

Hamid, G.; Khan, N. A.; Mohsin, S. I., & Meynell, P. J. (2000). Impact of sedimentological processes on mangrove ecosystem of the Indus Delta. Pakistan Journal of Marine Sciences, 9(1-2), 1-15.

Hecht, J. E. (Ed.). (1999). The economic value of the environment: Cases from South Asia. IUCN--The World Conservation Union.

Hinkel J., and Klein R. J. T. (2013). Coastal flood damage and adaptation costs under 21st century sea-level rise. PNAS, Proceedings of the National Academy of Sciences, 111(9): 3292–3297.

Horton, R., Herweijer, C., Rosenzweig, C., Liu, J., Gornitz, V., & Ruane, A. C. (2008). Sea level rise projections for current generation CGCMs based on the semi-empirical method. Geophysical Research Letters, 35(2).

IPCC. (2007). Fourth Assessment Report on Global Status of Climate.

Ismail, S.; Saifullah, S. M., & Khan, S. H. (2014). Bio-Geochemical studies of Indus Delta mangrove ecosystem through heavy metal assessment. Pak. J. Bot, 46(4), 1277-1285.

IUCN. (2002). Regional Technical Assistance for Coastal and Marine Resources Management and Poverty Reduction in South Asia: Situation Analysis Report, RETA 5974- PAK, Asian Development Bank and the International Union for Conservation of Nature.

IUCN. (2003), Environmental degradation and impacts on livelihoods sea intrusion, – A case study, IUCN Pakistan, 1-77.

Kalhoro, N. A.; He, Z.; Xu, D.; Faiz, M.; Yafei, L. V.; Sohoo, N., & Bhutto, A. H. (2016). Vulnerability of the Indus River Delta of the North Arabian Sea, Pakistan. Global NEST journal, 18(3), 599-610.

Khan, M. Z., and Akbar, G. (2012). In the Indus delta it is no more the mighty Indus. River Conservation and Management, 69-78.

Khan, N.M; Rastoskuev, V. V.; Sato, Y; Shiozawa, S. (2005). Assessment of hydro saline land degradation by using a simple approach of remote sensing indicators. Agric. Water Manage., 77(1-3): 96-109.

Khan, N. M.; Rastoskuev, V. V.; Shalina, E.V. and Sato, Y. (2001). Mapping salt-affected soils using remote sensing indicators-a simple approach with the use of GIS IDRISI. 22nd Asian Conference on Remote Sensing, 5(9).

Kirshen, P.; Watson, C.; Douglas, E.; Gontz, A.; Lee, J., & Tian, Y. (2008). Coastal flooding in the Northeastern United States due to climate change. Mitigation and Adaptation Strategies for Global Change, 13(5-6), 437-451.

Laghari A.; Abbasi, H.; Aziz, A.; Kanasro, N. (2015). Impact Analyses of Upstream Water Infrastructure Development Schemes on Downstream Flow and Sediment Discharge and Subsequent Effect on Deltaic Region. Sindh University Research Journal-SURJ (Science Series), 47(4): 805-808

Leichenko, R. M., & Wescoat Jr, J. L. (1993). Environmental impacts of climate change and water development in the Indus delta region. International Journal of Water Resources Development, 9(3), 247-261

Lichter M.; Vafeidis A.T.; Nicholls R.J.; Kaiser G. (2011). Exploring Data-Related Uncertainties in Analyses of Land Area and Population in the "Low-Elevation Coastal Zone" (LECZ). Journal of Coastal Research, 27: 757–768

Majeed, S.; Zaman, S. B., Ali, I.; Ahmed, S. (2010). Situational Analysis of Sindh Coast Issues and Options. Managing National Resources for future Agriculture, Research Briefings, 2(11).

McGranahan, G.; Balk, D.; Anderson, B. (2007). The rising tide: assessing the risks of climate change and human settlements in low elevation coastal zones. Environment and Urbanization, 19: 17–37.

Meehl, G. A., et al. (2007). Global climate projections, in Climate Change 2007: Contribution of Working Group I to the Fourth Assessment Report of the IPCC, edited by S. Solomon et al., pp. 747– 846, Cambridge Univ. Press, New York.

Memon, A. A. (2005). Devastation of the Indus river delta. In Impacts of global climate change (pp. 1-12).

Miller, L., and Douglas, B. C. (2004). Mass and volume contributions to twentieth-century global sea level rise. Nature, 428(6981), 406.

Mimura, N. (2008). Asia-Pacific coasts and their management: States of Environment (Vol. 11). Springer Science & Business Media. Springer, The Netherlands.

Meynell, P. and Qureshi, T. (1993). Sustainable management of mangroves in the Indus Delta, Pakistan, in David, T. (ed) Towards the Wise Use of Wetlands, Ramsar Bureau, Gland.

Neumann B., Vafeidis A. T., Zimmermann J., Nicholls R. J. (2015). Future Coastal Population Growth and Exposure to Sea-Level Rise and Coastal Flooding—A Global Assessment. PLoS ONE, 10(3): e0118571.

Nicholls R. J. (2004). Coastal flooding and wetland loss in the 21st century: changes under the SRES climate and socio-economic scenarios. Global Environmental Change, 14: 69–86.

Peracha, M. A., Hussain, M., Khan, N., Ali, M. L., & Khan, M. (2015). Degradation of Mangroves Ecosystem of Indus Delta. International Journal of Scientific & Technology Research, 4(8): 106-108.

Pessoa, L.G.M., Maria, B.G.D.S.F., Freire, D.S., Wilcox, B.P., Green, C.H.M., Araujo, R.J.T.D., & Filho, J.C.D.A. (2016) Spectral reflectance characteristics of soils in northeastern Brazil as influenced by salinity levels. Environmental Monitoring and Assessment, 188: 616.

Rasul, G., Mahmood, A., Sadiq, A., & Khan, S. I. (2012). Vulnerability of the Indus delta to climate change in Pakistan. Pakistan journal of meteorology, 8(16): 89-107.

Renaud, F. G., Syvitski, J. P., Sebesvari, Z., Werners, S. E., Kremer, H., Kuenzer, C., ... & Friedrich, J. (2013). Tipping from the Holocene to the Anthropocene: How threatened are major world deltas? Current Opinion in Environmental Sustainability, 5(6), 644-654.

Rohling, E. J., Grant, K., Hemleben, C. H., Siddall, M., Hoogakker, B. A. A., Bolshaw, M., & Kucera, M. (2008). High rates of sea-level rise during the last interglacial period. Nature Geoscience, 1(1), 38.

Sánchez-Triana, E., S. Enriquez, B. Larsen, P. Webster, and J. Afzal. 2015. Sustainability and Poverty Alleviation: Confronting Environmental Threats in Sindh, Pakistan. Directions in Development Series. Washington, DC: World Bank.

Schneider, S. H.; Semenov, S.; Patwardhan, A.; Burton, I.; Magadza, C.H.D.; Oppenheimer, M. et al. (2007). "Assessing key vulnerabilities and the risk from climate change," in Climate Change: Impacts, Adaptation and Vulnerability. Contribution of Working Group II to the Fourth Assessment Report of the Intergovernmental Panel on Climate Change, eds M. L. Parry, O. F. Canziani, J.P. Palutikof, P.J.vander Linden and C.E. Hanson (Cambridge, UK: Cambridge University Press),779–810.

Siyal, A. A., Dempewolf, J., & Becker-Reshef, I. (2015) Rice yield estimation using Landsat ETM+ Data. Journal of Applied Remote Sensing, 9(1), 095986-1-095986-16.

Sohl, M. A., Mehmood, A., Saeed, U., & Rafique, H. M. (2006). Temporal Mapping and Prediction of Coastal Biomass for Keti Bundar. Terra, 2, 5-192.

Spalding M, Kainuma M, Collins L (2010) World Atlas of Mangroves. Earthscan.

Steffen, W., Hunter, J., & Hughes, L. (2014). Counting the costs: Climate change and coastal flooding. Climate Council of Australia.

Sultana, J., Syed, J. H., Mahmood, A., Ali, U., Rehman, M. Y. A., Malik, R. N., & Zhang, G. (2014). Investigation of organochlorine pesticides from the Indus Basin, Pakistan: sources, air–soil exchange fluxes and risk assessment. Science of the Total Environment, 497, 113-122.

Syvitski, J. P., Kettner, A. J., Overeem, I., Giosan, L., Brakenridge, G. R., Hannon, M., & Bilham, R. (2013). Anthropocene metamorphosis of the Indus Delta and lower floodplain. Anthropocene, 3: 24-35.

Syvitski, J. P.; Vörösmarty, C. J.; Kettner, A. J.; Green, P. (2005). Impact of humans on the flux of terrestrial sediment to the global coastal ocean. Science, 308(5720): 376-380.

Salik, K. M., Hashmi, M. Z. U. R., & Ishfaq, S. (2016). Environmental flow requirements and impacts of climate change-induced river flow changes on the ecology of the Indus Delta, Pakistan. Regional Studies in Marine Science, 7, 185-195.

Van de Sande, B., Lansen, J., & Hoyng, C. (2012). Sensitivity of coastal flood risk assessments to digital elevation models. Water, 4(3): 568-579.

Vermeer, M., and Rahmstorf, S. (2009). Global sea level linked to global temperature. Proceedings of the national academy of sciences, 106(51), 21527-21532.

Wood, A., Pamela, S., Johanna, M. (2013). The root causes of biodiversity loss Pakistan Mangroves. pp. 257–261.

World Bank. (2019). Pakistan getting more from water. The World Bank Group. Washington, DC 20433, USA.

WWF (2010) Indus Delta Pakistan. WWF International: Gland, Switzerland. http://wwf.panda.org/what_we_do/where_we_work/indus_delta/ (visited on Jan. 24, 2019)

WWF. (2007). Indus Delta: a vanishing ecosystem. Indus for All Program, WWF – Pakistan, Regional Office, Karachi.

Yu, J., Li, Y., Han, G., Zhou, D., Fu, Y., Guan, B., ... & Wang, J. (2014). The spatial distribution characteristics of soil salinity in coastal zone of the Yellow River Delta. Environmental earth sciences, 72(2), 589-599.